



Subject Areas:

Volcano, Geophysics, Volcanic gases

Keywords:

InSAR, seismicity, volcano

Author for correspondence:

Matthew E. Pritchard

e-mail: pritchard@cornell.edu

Thoughts on the criteria to determine the origin of volcanic unrest as magmatic or non-magmatic

M. E. Pritchard¹, T. A. Mather², S. R. McNutt³, F. J. Delgado¹, and K. Reath¹

¹Department of Earth and Atmospheric Sciences, Cornell University, Ithaca, NY 14850 USA

²Department of Earth Sciences, University of Oxford, Oxford, UK

³University of South Florida School of Geosciences, 4202 E. Fowler Avenue, NES 107, Tampa, Florida 33620, USA

As our ability to detect volcanic unrest improves, we are increasingly confronted with the question of whether the unrest has a magmatic origin ("magma on the move") or a non-magmatic origin from a change in the hydrothermal system ("fluids that are not magma on the move") or tectonic processes. The cause of unrest has critical implications for the potential eruptive hazard (e.g., used in constructing Bayesian Event Trees), but is frequently the subject of debate, even at well-studied systems. Here we propose a set of multi-disciplinary observations and numerical models that could be used to evaluate conceptual models about the cause of unrest. These include measurements of gas fluxes and compositions and the isotopic signature of some components (e.g., H₂, He, C, SO₂, H₂O, CH₄ and CO₂), the spatial and temporal characteristics of ground deformation, thermal output, seismicity, changes in gravity, and whether there is topographic uplift or subsidence spanning hundreds-thousands of years. In several volcanic systems, both magmatic and non-magmatic unrest is occurring at the same time. While none of these observations or models is diagnostic on its own, we illustrate several examples where they have been used together to make a plausible conceptual model of one or more episodes of unrest and with whether eruptions did or did not follow the unrest.

1. Introduction

This special issue explores an emerging conceptual model of trans-crustal magmatic systems (TCMS) where magma storage and differentiation occurs at several locations throughout the entire crustal column [1,2]. This conceptual framework is being driven by petrological, geochronological, and geochemical studies of magma storage conditions that show (1) many large eruptions tap multiple melt sources, (2) large melt bodies are probably transient features, and (3) crystals carried by the transporting melt have been stored at a range of pressures and temperatures [2–4]. The implications of the TCMS model for eruption dynamics and forecasting are still being explored [1]. In particular, observations such as ground deformation, seismicity, and volcanic degassing are the basis of volcano monitoring, and interpretations of these data need to be reassessed within the newly-developed framework [1].

For example, most eruptions are presaged by at least a few days to weeks of volcanic unrest [5,6] – how does this unrest relate to the TCMS paradigm? However, some volcanic eruptions have little to no measured unrest before eruption [7,8] – is this consistent with the TCMS conceptual model? We define volcanic unrest "as the deviation from the background or baseline behaviour of a volcano towards a behaviour which is a cause for concern in the short-term because it might prelude an eruption" from Phillipson et al., (2013) [6]. Given this definition, since the level of background activity varies for each volcano, the threshold for unrest is determined separately for each volcano [9]. However, while the unrest "might prelude an eruption," unrest may not result in an eruption at least in the short term – these events are sometimes called "failed eruptions" [10]. According to the TCMS paradigm [1], unrest can be both magmatic and/or non-magmatic (Fig. 1a,b) – caused by destabilization of magma layers, volatile accumulations, or both. Unrest can result in eruption or not depending on the size, location, and rapidity of the destabilization (Fig. 1c), possibly involving multiple layers [1]. To assess the eruptive threat from a given episode of unrest, it is critical to understand its origin. If unrest is caused by magma layer destabilization and movement, Sparks and Cashman (2017) consider it more ominous than volatile accumulation and release from magma that moved during a previous destabilization, or changes in the shallow hydrothermal system [1].

To quantify the possible eruptive threat from unrest episodes, several groups have developed Bayesian Event Trees (BET, Fig. 2) that include an assessment of the likelihood that the unrest is caused by "magma on the move", geothermal or tectonic activity, or some other process [9,11–13]. The eruption hazard from non-magmatic unrest (geothermal, tectonic, volatile accumulation and release, or other) is generally lower than magmatic unrest. But, these event trees include the possibility of hazards from non-magmatic unrest, including eruptions, for example through sector collapse, phreatic explosions, or a tectonically induced fracture [11,12]. Non-magmatic unrest includes "fluids on the move" [13], where the fluids include brines, gas, supercritical fluids or a combination of these as long as partially molten rock (magma) is not migrating [13]. These fluids could have their origin from magma, for example volatiles derived from stagnant [9] cooling/crystallizing magma batches (e.g., Fig. 1a,b) and are called "magmatic fluids" [14], from meteoric/groundwater water mixing in the hydrothermal system, or a combination of the two that are referred to as "hydrothermal fluids." This distinction between magmatic and non-magmatic unrest is not yet standardized. For example, a comprehensive review of global caldera unrest between 1984–2014 noted that when known, the root cause for all unrest at calderas was magmatic [15]. By the definitions used here, not all of these caldera unrest episodes are from "magma on the move." Using BET allows the simultaneous consideration that unrest could be magmatic or non-magmatic when evaluating the outcomes of the unrest episode.

To implement BET frameworks such as those shown in Fig. 2, the top level question for evaluating hazard from an unrest episode is determining the probability that unrest signifies magmatic or non-magmatic processes. Specific monitoring criteria that can distinguish between the origins of unrest have been proposed at a few volcanic systems (Table 1) [13]. Yet, this is a challenging question to answer, as there has been a long history of debate about magmatic

vs. non-magmatic sources of unrest even at well studied volcanoes [14,16]. On the other hand, our ability to monitor unrest on a global basis is increasing thanks to a growing number of space and ground-based observations [17,18], and the exposure of global populations to volcanic hazards [19] motivates improved assessment of the origin of volcanic unrest. Our goal in this paper is to review the characteristics of unrest that could be diagnostic of magmatic or non-magmatic processes and present some case studies where these characteristics have been used to develop conceptual models of the causes of unrest. Certainly, the TCMS paradigm reinforces the idea that both magmatic and non-magmatic unrest could be occurring at the same time [20], but we suggest that the critical question is still whether there is evidence for "magma on the move" irrespective of evidence for additional hydrothermal activity. We propose a check-list of criteria that could be consulted during new episodes of activity to assess the origin of unrest and prioritize new diagnostic observations. Our focus is on silicic systems because these are the sites of the most explosive and dangerous eruptions on Earth, but we include some useful examples from other systems as well.

2. Methods: Types of data to distinguish cause of unrest

In this section we review monitoring criteria that have been used to assess whether unrest is magmatic or non-magmatic. None of these non-eruptive criteria are unique – the best way to determine if unrest is magmatic is to see if it culminates in an eruption of new magma. This is necessarily retrospective. But unrest due to "magma on the move" doesn't always result in eruption [10]. In practice, no single non-eruptive criterion is used to determine if unrest is magmatic [13]. For some volcanoes, there is a history of relating unrest to eruption, so there may be specific quantitative thresholds that can be used to assess the likelihood that unrest is magmatic (e.g., Popocatepetl and Cotopaxi, Table 1). However, since these criteria are specific to each volcano, we do not attempt to assign quantitative values – instead we discuss the value and qualities of the different types of data. The use and combination of these data-streams to assess the nature of unrest is explored further in the case studies in section 3.

(a) Gravity change

A key difference between magmatic and non-magmatic fluids is that their density differs by a factor of 50% or more – thus measurements of gravity change associated with unrest that determine the density of the moving fluids could be used to diagnose the cause of unrest if the mass change is large enough [21]. Gravity change has been reported at several volcanoes with fluid densities ranging from 142–1115 kg m⁻³ (likely water and/or gas) [22,23] to 2192–3564 kg m⁻³ (partially molten rock) [24,25] to a combination of the two between 1000–2500 kg m⁻³ [26,27]. Ground deformation is often, but not always associated with gravity change – differences between the source of gravity change and deformation can illuminate the origin of unrest [28]. Gravity measurements are difficult to make and several corrections must be applied in order to infer the density values – for example, changes in aquifer levels impact the surface gravity and are not always well constrained [21,24]. There are only a few locations where density values (Long Valley and Yellowstone, USA and Corbetti, Ethiopia) [24,26,29] or the combination of gravity and deformation data (Kilauea, USA and Etna, Italy) [28,30,31] require injection of new magma. However, the inference of magma injection at Long Valley, one of the best cited studies of this kind, has recently been questioned [32] on the basis that the observed gravity changes could be related to variations in groundwater or other errors. For example, the gravity change attributed to magmatic injection ($66 \pm 11 \mu\text{gal}$) [26], is similar to the gravity signal in areas not undergoing deformation ($52 \pm 22 \mu\text{gal}$) and outside the caldera ($66 \pm 20 \mu\text{gal}$) [32].

Unfortunately, microgravity surveys are limited by significant spatio-temporal aliasing compared with other field techniques [21]. This aliasing arises from the high price of the instruments which does not allow for frequent deployment of a network of continuous instruments. Where collected, continuous gravity observations (see summary in [21]) reveal large

short-lived signals related to hydrothermal activity, such as at Nisyros, Greece [33] and eruptive activity at Kilauea, USA and Etna, Italy [28,34]. But these types of data are rarely available. Further advances in continuous microgravity require new types of low cost instruments [35], similar to GPS and seismic stations.

(b) Ground deformation

Ground deformation can be caused by magmatic or non-magmatic unrest [1,36]. But several spatial and temporal characteristics of the deformation, as well as the relation of deformation changes to coincident or delayed changes in other data types (e.g., seismicity, gravity, and degassing) could be more diagnostic for the origin of unrest. Here, we briefly describe a few of these deformation characteristics.

Size of deformation/Depth of source: The size of the deforming region is related to the size and/or depth of the source. A deeper source causes deformation over a larger area of the surface, but the deformation pattern is non-unique – a large shallow source could also match the data. If there is additional data from petrology and/or other geophysical methods, the source depth can be better constrained [37]. Because hydrothermal systems are usually <10 km deep [38], source depths greater than this likely indicate magmatic unrest. But it is possible that magmatic fluids at depths >10 km are the source of unrest without "magma on the move" [39] as part of the TCMS model [1].

Relation to degassing and seismicity: At several volcanoes, ground deformation changes rate and even direction over short time periods (days to years) and these changes are correlated with changes in seismicity and degassing that can be used to diagnose the origin of unrest [14,20,40]. We will discuss how these different datasets can be combined together below in the case studies for individual volcanoes (section 3).

Relation to geomorphic uplift: The repose interval between eruptions is frequently hundreds to thousands of years (or longer), and it may take a similar amount of time to accumulate magma between eruptions. Over these timescales, geomorphic uplift can provide a record of magma injection. These geomorphic observations complement the shorter duration geodetic observations spanning years-decades, but are limited to areas where geomorphic features are created (e.g., shorelines, river and coastal terraces, etc.) and preserved. In fact, uplift of tens to hundreds of meters has been recorded in some volcanic areas over the past centuries to millennia and have been related to magmatic unrest without eruption (e.g., Laguna del Maule, Chile; Ioto (Iwo Jima), Japan; Socorro, New Mexico) [41–43]. There is at least one example of 20 m of uplift being related to non-magmatic unrest in the Gulf of Naples [44]. On the other hand, there are also examples of volcanic areas that have little geomorphic uplift (less than a few tens of meters) despite significant or persistent geodetic deformation rates [45–47]. The inference is that these geodetic rates are not sustained for centuries or millennia, such that the deformation is caused by transient magmatic unrest or episodic non-magmatic unrest [45–47].

Temporal evolution of ground deformation: Several different types of analytic and numerical models can be used to assess if unrest detected by ground deformation is of magmatic or non-magmatic origin. While these models are non-unique, they are useful for developing testable hypotheses about the nature of unrest. For example, ground deformation signals at several silicic [48–51] and basaltic [52–56] volcanoes show either exponential or a double exponential pattern in time. These signals are predicted by several models that couple Newtonian magma flow in a conduit from a deep pressurized source (usually in the lower crust) into a shallow pressurized reservoir. Variations of the coupled reservoir-conduit models incorporate two coupled shallow reservoirs [55] and reservoirs surrounded by a viscoelastic media [57]. The exponential and double exponential patterns arise from the deep source pressurization function. A deep source pressurization increase followed by a constant pressure results in a double exponential, while a deep source constant pressure results in a single exponential. The quasi-exponential trends in ground deformation data can thus indicate magma injection but can also be caused by reservoir pressurization in a viscoelastic media. The ambiguity between these interpretations can be

addressed by numerical simulations which show that in some volcanoes the viscoelastic response is of secondary importance with respect to the transient magma injection [49,58–60].

Ground deformation can also be caused by movement of non-magmatic multiphase (liquid, gas, super-critical fluids) and multicomponent (e.g., $\text{H}_2\text{O}-\text{CO}_2$) hydrothermal fluid flow and poroelastic deformation [61–63]. The diagnostic rates, patterns, total magnitudes, and durations of ground deformation from these non-magmatic models can be similar to magmatic models of ground deformation [61], and so other types of data (gravity, seismicity, gas, etc.) are important in distinguishing the cause of ground deformation. Unfortunately, these models have been rarely used to predict ground deformation time series. Instead of modeling the temporal evolution, most of the ground deformation studies have only used a set of either cumulative or average displacements. Hence, the potential ability to assess whether the exponential or double exponential signals result from magma injection or hydrothermal flow for time scales of 1–10 years is still an area of active research.

(c) Temperature

Some volcanoes and fumarole fields (e.g., Momotombo, Nicaragua [64]; Satsuma-Iwojima, Japan [65,66]; Kudryavy, Kuril Islands [67]) have continuous high temperatures at the surface (700–900°C) that imply shallow magma, but without evidence of magma migration [9]. In some cases, these high temperatures have been ongoing for decades to centuries, and crystallization and/or convection of a stagnant magma body can explain the degassing and high surface temperatures [9]. Globally, there are dozens of such stagnant, but degassing magma bodies (e.g., Pleistocene restless volcanoes and calderas with fumaroles and sometimes ground deformation and seismicity [68]), that may be considered in a "dormant" state (Fig. 1) [1]. On the other hand, spatially large and high temperature thermal anomalies that produce incandescence at the summit, for example eruptions at Popocatépetl, Mexico (Table 1) and the lava lakes, such as that at Villarrica, Chile [69], can indicate magmatic unrest near the surface. Transient increases in temperature and area of the fumarole field provide more ambiguous evidence of magmatic or non-magmatic sources. Sandri et al., (2017) [13] notes that at some volcanoes, temperature increases of 120–200 °C are hydrothermal (non-magmatic) and increases >300 °C are magmatic. Kern et al., 2017 [70] describes the thermal detection of the increase in area of the fumarole field and the increase of water vapor degassing before the 2016 eruption of Sabancaya. The increase of water vapor can clearly be related to "fluids on the move" but it is unclear if the driving force to originally cause fluid movement was the introduction of new magma (i.e., "magma on the move").

(d) Seismicity

At some volcanoes, particularly long-dormant ones, swarms of volcano-tectonic (VT) earthquakes may occur before other signs of unrest or before there is a clear sign that the unrest is of magmatic origin. For example, unrest at Cerro Chiles, Ecuador-Colombia [71] and Sabancaya, Peru [72] started as earthquake swarms with an unclear magmatic connection, but as time progressed, evidence for magmatic intrusion developed in both locations.

Swarms of VT earthquakes are common at volcanoes – that is many earthquakes of about same size that happening within the same volume over a short duration [73]. However, an informal poll of experts estimates that only about 1/3 to 1/10 of swarms precede eruptions (McNutt, unpublished data). The idea is that over time, numerous swarms occur, but only a fraction of them are followed immediately by eruptions. These values would be initial probabilities of the first branch of BET (a more formal elicitation or similar study is needed to yield further insights). The low rate of precursory swarms (or high rate of false alarms or intrusions) is broadly consistent with the TCMS model. Magma may move between different components of TCMS but swarms are not necessarily pre-eruptive. VT swarms typically have rates about one order of magnitude above background, and swarm durations range from hours to months or more with a mean of

about 5.5 days [73]. Pre-eruptive swarms have systematically longer durations by about a factor of two [73].

A systematic pattern of seismic event types has been observed and has been described as the Generic Volcanic Earthquake Swarm Model (GVESM [74]). The sequence consists of VT events that reach a peak rate of occurrence, followed by relative quiescence. Next to appear are low-frequency (LF) events (also called long-period or LP) followed by tremor. LF events and tremor often have similar frequencies (1-5 Hz) and are thought to represent transient (LF) and sustained (tremor) fluid processes in sections of conduits at shallow depths. The fluids may be magma, water (e.g. groundwater), gases, or any combination of these. An uptick in seismicity often precedes eruptions on a time scale of hours; this may be VT or LF events or an increase in tremor amplitude. Strong tremor generally accompanies eruptions with the amplitude (using a metric known as reduced displacement) being roughly proportional to the VEI [75]. Swarms of deeper VT events often follow eruptions as stresses re-adjust in the vicinity of magma chambers. The time frames of swarms that follow the GVESM are highly variable; examples are given in [74].

Not every earthquake swarm at volcanoes follows the GVESM sequence. There are cases of some elements missing; for example, the Redoubt 1989 sequence was missing VT events, and instead had LP events, tremor, and the onset of eruption 23 hours after the LP events began [76]. Presumably the deeper ascent of magma from 10 to 1 km was relatively aseismic.

The GVESM is a conceptual model that is consistent with vertical ascent of magma and/or volatiles. Most VT events occur at depths of 3-10 km whereas LF events occur at depths of 1-3 km and tremor even shallower. Observations of increased steaming are common around the time of LF event onset. A complication is that a water/gas front may rise in advance of the magma, and this would also give the observed sequence of events. If the tremor and/or LF events are caused by boiling of hydrothermal waters, the reduced displacement is generally less than 5 cm^2 [77,78]. Eruption tremor (magma) is considerably stronger.

In addition to the increased rate of events that makes up a swarm, the distribution of event sizes may also change. Seismologists refer to this as the frequency-magnitude distribution or b-value (b is the slope in the relation $\text{Log}_{10} N = a - bM$, where N is cumulative number of events, M is magnitude, and a and b are constants). Laboratory studies show that b increases (steeper slope or more small events) with higher pore pressure or thermal gradient, and decreases (shallower slope or more large events) with higher stresses. Thus b -values can shed further light on processes and likelihood of eruption. For example, the 2006 Augustine eruption was preceded by a decrease in b -value months before it began [79].

In terms of BET scenarios, VT swarms alone likely give probabilities of eruption of 1/10 to 1/3 as mentioned above. If the b -values become lower, this suggests increased magmatic pressure. If VT events are followed by LF events, the probability of an eruption (i.e., a magmatic origin) increases, although it is hard to be more quantitative at this stage. An increase in b -value at this point could indicate either increased pore pressure (hence water) or increased thermal gradient (magma or water). The probability increases again with the onset of volcanic tremor. So overall, the presence of different types of events, which forms the basis of indicating adherence to the GVESM, suggests a higher likelihood of eruption than the presence of any one type of seismicity alone. However, the presence of the GVESM sequence does not unambiguously show that magma or water or gases are the cause. Additional characteristics of the seismicity can help resolve the ambiguity. For example, a recent paper by Passarelli et al. (2018) [80] determined that lateral magmatic dike intrusion was the most likely cause of a swarm at Jailolo volcano. This was based on careful assessment of hypocenter migration, focal mechanisms, non-double-couple components, surface fracture orientation, and tectonic considerations.

Deep long-period (DLP) events are also recorded at volcanoes. At some volcanoes their rate of occurrence is approximately steady state, such as Kilauea [81] even though surface eruptive activity is intermittent. Models of DLP events and tremor generally involve fluid (could be magma or not) movement through constrictions in dikes or sills. At some volcanoes DLP events are precursors. For example, DLP events appeared about 2 weeks before the 1991 eruptions

of Pinatubo, although they were only recognized in hindsight [82]. At other volcanoes, DLP events mostly occurred after eruptions, such as at Mount Spurr in 1992 [83]. All three cases cited here suggest the involvement of magma. However, DLP events beneath Mammoth Mountain, California, have been linked to CO₂ release at the surface that may or may not be related to "magma on the move" [84]. Many DLP events in the Cascades, Japan, and Alaska are not associated with eruptions or unrest.

Another class of earthquakes is known as very long-period (VLP) events. The period is 10 seconds or longer (up to 50 seconds) and both shallow and deeper events have been recorded. Two well-studied examples are at Stromboli, Italy associated with gas slug motion through magma [85], and at Aso, Japan associated with expansion and contraction of a shallow geothermal feature [86]. Again similar seismograms are recorded with and without magma involvement.

Intrusion and pre-eruption swarms share common features with the exception of shallow harmonic tremor near the eruption site when an eruption is the outcome of unrest [87]. This suggests that intrusions represent the same suite of processes as pre-eruptive swarms but the magma stalls before reaching the surface (see also [10]).

(e) Gas flux and composition

Magmas at depth have numerous chemical species dissolved within them that exsolve as magma rises through the crust. The major gas species are usually H₂O, CO₂, SO₂, H₂S and the halogen halides (e.g., HF, HCl) but other minor components include noble gases (e.g., He), H₂, CH₄, CO, COS and metallic species. The composition of the gas mixture will depend on factors including the pressure of release of the gas (e.g., CO₂ tends to be exsolved deeper in the crust than other species and higher pressures favour H₂S over SO₂), the temperature of the system, mixing between magmatic and other volatile sources and interactions with ground water or hydrothermal systems that might strip or scrub out soluble species [88,89].

Where present, gas emissions at restless volcanic systems can be characterized by a range of surface manifestations. In some (usually basaltic) systems like Etna (Italy) and Villarrica (Chile) gas is emitted from a magma-air interface at a visible lava lake or down within the vent/conduit. Other systems are characterized by fumarolic emissions, hot springs, emissions through lakes or diffuse seeping out as soil gas.

As SO₂ emissions from a magma occur at a lower pressure than CO₂ and are favoured by high temperature and low pressure conditions, an increase in SO₂ flux at a volcano may herald the arrival of new magma into the shallow system. For example, SO₂ flux measurements were an important contributor to successful prediction of the June 1991 eruption of Mount Pinatubo. Measurements in mid-May (500 tonnes/day) indicated that unrest involved intrusion of magma. By late May the flux had increased tenfold, interpreted to imply that (1) magma was rising and/or (2) a hydrothermal system was being boiled and removed, allowing more of the SO₂, that had previously been scrubbed by it, to reach the surface. Both of these scenarios pointed to an increased hazard from the volcano. The signals were not always straightforward to interpret, however. On 5 June there was a sudden, short-lived drop in SO₂ flux (to 260 tonnes/day), even as seismicity was increasing. This may have been caused by plugging or sealing of the system inhibiting gas escape. On June 7, as a new dome was extruded, emissions increased again and the last pre-paroxysmal measurement (10 June) was >13,000 tonnes/day [90].

Changes in SO₂/CO₂ ratios have been suggested to be of use to forecast magma movement and hence dangerous unrest resulting in explosive eruptions at both systems with strong hydrothermal processing (e.g., the gas emissions through the lake at Poás volcano, Costa Rica in 2014 [91]) and the more dominantly magmatic emissions from systems like Villarrica, Chile [92], Etna and Stromboli volcanoes, Italy [93,94]. However, these systems go through long periods of unrest with known magmatic involvement and these studies are more aimed at finding precursors to dangerous changes in this background unrest rather than establishing whether or not there is a degree of magmatic involvement. Gas fluxes and ratios were also used to give key insights into the deep processes occurring during the 2010 explosive eruption of Merapi volcano in Indonesia.

Increases in CO_2/SO_2 and $\text{H}_2\text{S}/\text{SO}_2$ over the months prior to the eruption recorded in fumarole gas samples, were used to suggest a deep degassing source associated with an input of fresh magma (most likely of mafic composition). The quantity of SO_2 degassed was used to argue for the presence of an exsolved fluid phase in the pre-eruptive magma body, which could have played a key role in the eruption's explosivity [95]

The presence of SO_2 and HCl , clearly magmatic gases, does not necessarily imply the migration of a magma though, as exsolution of both species can occur through convection in the magmatic plumbing system and/or crystallization of a stagnant, cooling magma batch and gas exsolution [9]. For example, Kawah Ijen, Indonesia has mainly been in a state of non-magmatic unrest for years, with the occurrence of only phreatic or geyser-like eruptions [38]. Nevertheless, the volcano hosts the largest reservoir of acidic surface water on Earth, continuously fed by the input of magmatic gases and volatilized metals [9].

At many systems, such as caldera systems, that start to show new unrest after periods of quiescence, the surface manifestations in terms of degassing might, at least initially, be more subtle and build up more slowly than in cases like Pinatubo. In cases where diffuse emissions of gases emitted deeper in the Earth's crust dominate (usually CO_2 dominated) scientists are left with the challenge of determining changes in degassing fluxes and patterns where emissions are over large spatial areas (e.g., Mammoth Mountain, USA [96]). Compositional changes such as in carbon or helium isotopes measured in diffuse or fumarolic gases can offer key evidence for the arrival of new magma with $\delta^{13}\text{C}\text{-CO}_2$ of -4 to -8 ‰ and $^3\text{He}/^4\text{He} > 3 \text{ Ra}$ (where Ra is the atmospheric value of $^3\text{He}/^4\text{He}$) thought to be characteristic of deep magmatic/mantle values [97,98]. Changes in composition with respect to concentrations of gaseous species like CO , H_2 and CH_4 are interpreted to indicate temperature changes within the system, which again may indicate the arrival of new magma [99,100].

(f) Hydrothermal activity: Water Flux and Chemistry, and Heat Flow

Changes in the hydrothermal system including the inter-related observations of heat flow, water flux and chemistry can be caused by both magmatic and non-magmatic unrest. Several silicic systems like Campi Flegrei, Long Valley and Yellowstone have large hydrothermal systems. However, not every volcano has a large hydrothermal system clearly linked to the magmatic system like Laguna del Maule and Lastarria-Lazufre (described in section 3). In Iceland, for example, there is no significant hydrothermal system at Hekla, indicating that any significant partially molten volume is deep ($> 14 \text{ km}$) [101]. However, Krafla and Grimsvotn support hydrothermal systems and shallower magma [101]. It might seem obvious that if there is no surface manifestation of a hydrothermal system, then hydrothermal activity could not be a source of unrest, and a magmatic origin for the unrest is more likely. However, further investigation is required since there are "blind" geothermal systems. In these systems, near-surface permeability conditions do not allow a hydrothermal system to develop above a magmatic heat source, and the hot fluids are forced to move 10 or more km horizontally [102].

Water outputs from hydrothermal systems can manifest in numerous ways (e.g., hot springs, mud pools and volcanic lakes/streams) and their chemistry can be intimately linked to fumarolic gas chemistry (see section 2e). For example, volcano lake compositions are strongly influenced by volcano fluid inputs although modulated by meteoric inputs and physical, chemical and biological processes within the lake. These in turn might be dominated by magmatic gases or the products of their interactions with the edifice/crustal rocks during transport. Major variations in lake composition often result from a changing volcanic input composition or magnitude and are thus useful for volcano monitoring [103]. Similarly, thermal spring compositions are modulated by external inputs (e.g., meteoric water), magmatic fluids and interactions with the edifice and crustal country rock. Despite this complex interplay between sources modulated by feedbacks such as fluid pH and temperature changes in thermal spring chemistry and the resulting streams or rivers can be useful indicators of variations within the system [104,105]. In submarine systems, magmatic intrusions have been shown to change the He , CO_2 , H_2 and CH_4 , and the $^3\text{He}/\text{heat}$

ratio from hydrothermal fluid samples for months before returning to background levels over longer time periods [106].

A high heat flux at a volcano is ultimately driven by magmatic activity, but is also responsible for hydrothermal activity. The amount of interaction between the hydrothermal system and the magma below can be measured by monitoring the discharge in Cl from streams and constraining the heat flow [107]. Increased heating of the hydrothermal system and increased heat flux in general can indicate new magma in the system or increased transport of existing magmatic fluids, triggering further unrest [108]. Water flux variations have been seen in the water level of crater lakes after the El Chichón, Mexico eruption in 1982 and a rise in the lake at Poás, Costa Rica before eruption [9]. Such water level measurements are not frequently made. Changes in water levels can also be monitored by geophysical methods like self potential, microgravity, resistivity or other surveys [9].

(g) Drilling: Direct sampling and monitoring of the subsurface

The monitoring techniques mentioned so far (gas and water sampling, seismicity, temperature, ground deformation, gravity, etc.) are restricted to making measurements at the surface or in shallow boreholes [109,110], such that only inferences can be made about conditions at depth causing unrest. In a few cases, drilling several km into upper crustal magmatic and hydrothermal areas has directly measured parameters that are critical for developing numerical models: the composition, physical properties (e.g., density, permeability, thermal conductivity, etc.), stress state, and temperature at depths closer to where unrest is occurring [111]. Some of these wells were designed for primarily scientific objectives [112–115] whilst others were for geothermal energy development. In several cases, the drilling revealed features that were unsuspected based on surface data alone, like lower temperatures than expected [116] and very abrupt transitions between solid and partially molten rock [117–119]. To provide ground truth to our near-surface monitoring data (e.g., the location of sub-solidus conditions, super-critical fluids, partially molten rock, etc.) and develop numerical models, future drilling and installation of deep observatories have been suggested [120–122]. Such drilling would also better constrain the location and properties of high enthalpy geothermal systems that could be a high quality energy source [123].

3. Case studies: Combining data-streams to understand unrest

In the last section, we reviewed the general data-streams that have been used to estimate the likelihood that unrest is magmatic. In the following section, we briefly discuss nine specific cases where multiple of these criteria have been combined to assess the origin of unrest. This is not intended to be an exhaustive review of such studies but is rather intended to illustrate key points via examples from a range of volcanic systems. Our examples are determined by those systems where suitable studies exist, but are also chosen to span different tectonic settings (rifts, subduction zones, hotspots) as classified by [68] that have been shown to have different characteristic relations between ground deformation and eruption globally [124]. More examples of caldera systems and more detail on restless episodes are available in [15,38]. Here the focus is on how multiple parameters have been used to assess if unrest requires "magma on the move" (even without eruption) and what additional data are required to assess this. Some of these systems (like Campi Flegrei and Yellowstone) have been extensively discussed already in the literature and so we include briefer comments and references. We spend more time on lesser-studied systems where multi-parameter observations of the unrest are in the nascent stages of being synthesized into conceptual models of the magmatic system.

(a) Long Valley, USA – rift

Unrest at Long Valley, USA has been ongoing for almost 40 years without eruption and includes earthquakes, ground deformation (Fig. 3a), gravity change, degassing (including CO₂ flux

increases that killed trees) and changes to the hydrothermal system [32]. The unrest spans more than 20 km laterally from a large Pleistocene silicic caldera to the younger dacitic Mammoth Mountain and surrounding basaltic eruptions. The various manifestations of caldera unrest have been related to magma injection, but recently Hildreth (2017) [32] proposed that the unrest in different parts of the Long Valley system could have different causes. Specifically, the uplift, earthquakes and other activity in the Pleistocene caldera could be caused by degassing of stagnant magma (that he attributes to "second boiling") [32]. He questions whether the gravity change in the caldera that has been attributed to magma intrusion because of the high density [24,25] could not be due to non-magmatic processes (i.e., the gravity change "signal" is being misinterpreted because it is actually "noise"). On the other hand, he attributes the CO₂ flux and earthquakes beneath and near Mammoth Mountain to the intrusion of mafic magma. A lingering question at Long Valley is if the caldera uplift since 1980 (about 0.8 m) is related to gas pressurization, why has there not been subsidence of approximately equal magnitude as the uplift as seen at Yellowstone or at least appreciable subsidence as at Campi Flegrei (Fig 3)? One possibility is that the depressurization may take a longer time period than the available observations. For example, gas uplift of a dome (5 km diameter) of 20 m in the Gulf of Naples has been proposed to have lasted 12,000 years [125] – but the contrast with Yellowstone over the last decades where significant subsidence has occurred is striking (Fig 3). Over the last 333,000 years, uplift of the caldera as recorded in lake sediments and the Hot Creek flow is constrained to be of order 40 m [32]. Either the caldera uplift events like that over the last 40 years don't eventually lead to equal subsidence and are infrequent (i.e., repeat every ~ 8000 years) or are eventually counterbalanced by subsidence, consistent with non-magmatic unrest driven by cycles of nearly equal pressurization/uplift and depressurization/subsidence.

(b) Campi Flegrei, Italy – subduction zone

Campi Flegrei caldera has experienced several episodes of unrest (e.g., total ground uplift over 3 m, Fig. 3b) during the 20th century without eruption [15]. The caldera last erupted in 1538 and its activity is of great concern to the 360,000 people who live in the caldera and the 3 million residents of neighboring Naples [126]. There have been decades of discussion about whether unrest at Campi Flegrei is magmatic, non-magmatic, or both [16,22,125] and a comprehensive review of the relevant datasets and arguments is beyond the scope of this paper. Many studies have shown the value of combining multiple datasets when inferring the cause of unrest. One argument for a non-magmatic origin of unrest is the delay between increased diffuse degassing following the uplift pulses lasting about 100 days [127]. When combining geophysical and geochemical data time series spanning multiple decades (e.g., Fig. 3b), it is possible to see that different episodes of unrest have different characteristics and possibly different origins. Evidence for both magmatic and hydrothermal contributions to the unrest are suggested based on comparison of ground deformation and several other datasets [40,108]. However, there are different interpretations of the origin of individual episodes of unrest using combined geophysical and geochemical datasets. For example, Moretti et al. (2017) [125] argue that the 1982-1984 unrest is primarily magmatic while the unrest since 2005 is non-magmatic while other papers flip the interpretations for these two episodes [108,128]. Offsets in coastal features show episodic cycles of decimeter uplift and subsidence over decades-centuries related to a combination of magmatic and non-magmatic processes [129], including a permanent uplift of as much as 33 m inferred to be magmatic intrusion in the last 2000 years [130].

(c) Yellowstone, USA – hotspot

The Yellowstone caldera has an observational record of cyclic inflation and deflation (Fig. 3c) spanning almost a century [14]. Similar patterns of uplift and subsidence occur over millennia and have resulted in net geomorphic change of only a few tens of meters [45]. Changes in deformation from inflation to deflation are correlated with seismic swarms (Fig. 3c) and changes in the

hydrothermal discharges. Ground deformation in different parts of Yellowstone is frequently anti-correlated – when the Norris Geyser Basin changes from uplift to subsidence, the Sour Creek resurgent dome deformation has the opposite sense (Fig. 3c). The deformation sources responsible for the inflation and deflation cycles are located within the large body of partial melt that underlies the caldera, in both the shallower rhyolitic (depth $\sim 5\text{--}15$ km) and the deeper basaltic (depth $\sim 15\text{--}20$ km) sections of the tomographically imaged TCMS extending from the surface to the lower crust at depths of ~ 50 km, and with a volume of $\sim 56,000$ km³ [26,131,132]. That changes in deformation in different parts of the caldera occur together and rapidly (within a few days to weeks, for example in early 2014, Fig. 3c) suggests coupling of low viscosity fluids. The deformation overturn and seismic swarms are thought to be produced by the breaching of a sealed layer that mobilizes magmatic fluids in the shallow hydrothermal system [133]. The driving mechanism responsible for the broad caldera uplift is thought to be basaltic magma injection (related to a large CO₂ flux), cooling rhyolitic magma releasing fluids, and a significant contribution from hydrothermal processes. The exact coupling between the hydrothermal and magmatic systems and how much deformation is of hydrothermal origin is currently unknown [14]. Yet, the correspondence between the magnitude of inflation and deflation over years to millennia suggests a role for a recoverable process like pressurization and depressurization by fluids on the move, as opposed to persistent uplift expected from repeated magmatic intrusions [45].

(d) Central Andes: Uturuncu, Bolivia and Lazufre, Chile-Argentina – subduction zone

Two areas of ground uplift, seismicity, and other manifestations of unrest in the central Andes at Uturuncu, Bolivia and Lazufre, on the Chile-Argentina border are not obviously associated with recent eruptions [134]. Uturuncu is a dacitic stratovolcano of Pleistocene age and Lazufre is about 10 km from two Pleistocene-Holocene-age andesitic-dacitic arc volcanoes called Lastarria and Cordón del Azufre. A connection between the Lazufre magmatic system and the active hydrothermal system at Lastarria 10 km away is suggested [135–137], but not yet confirmed. Both Uturuncu and Lazufre-Lastarria are likely associated with TCMS spanning hydrothermal systems at the surface to geophysical anomalies (e.g., low electrical resistivity and low seismic velocities) indicating partial melt through the mid- to lower crust [134]. Unrest is occurring at multiple depths at approximately the same time within the system, and it has been proposed that unrest of magmatic origin is the cause of deep unrest [138,139] while non-magmatic activity may be the cause of shallower unrest [135,140,141]. A different interpretation is that all of the unrest is of non-magmatic origin and caused by cycles of vertical up and down movements related to volatile-driven pressurization and depressurization [39,134]. The non-magmatic origin would be consistent with no geomorphic uplift over thousands of years [47]. On the other hand, at Lazufre, there is evidence of ~ 500 m of uplift over the past 0.4 Ma that could be related to magmatic intrusions over the longer time period [47,135]. To further assess whether there is "magma on the move" at Uturuncu and Lazufre, analysis of seismic data at Lazufre (e.g., shallow and deep LP events) and measurements of gas at both Lastarria and Uturuncu are ongoing.

(e) Laguna del Maule, Chile – subduction zone

Laguna del Maule (LdM) is a large center of silicic volcanism in the southern Andes with significant unrest since at least 2007 (uplift of more than 20 cm/yr, earthquakes, gravity change) but no historic eruptions [142]. The ground uplift is modeled as an inflating sill at 4.5 km (magmatic unrest) [49], while the gravity change is primarily caused at shallower levels by low-density fluids (non-magmatic unrest) [23] that are not related to any known surface geothermal system, but such a system could be hidden beneath the lake or displaced 15 km (Baños Campanario [143]). The long-term geomorphic uplift of 60 m suggests repeated magmatic

intrusions over the last 20,000 years [42], and the absence of a shallow hydrothermal system also strongly suggests a role for magmatic unrest. LdM is another example (along with all examples cited so far) where magmatic and non-magmatic unrest are occurring at the same time at different locations in the TCMS.

(f) Cordón Caulle, Chile – subduction zone

Cordon Caulle (Southern Chile), is a ~10 km long large rhyolitic fissural system that has had three large rhyodacitic eruptions (VEI 3-5) in 1921-1922, 1960 and 2011-2012 with nearly the same chemical composition [144,145]. The volcano also hosts one of the largest hydrothermal systems in the Southern Andes, with several acid fumaroles and even a small geyser [146]. The 9-month 2011-2012 eruption is the only one with instrumental observations at this volcano, and was preceded by several years of InSAR-detected ground deformation from 2007- 2009 and early 2011 (Fig. 4a). Seismic observations are only available since mid 2010, and show a clear seismicity increase two months before the eruption [147], in agreement with the pre-eruptive ground deformation. Despite the seismic and deformation pre-cursors [145], there was no observed increase in temperatures of the fumarole fields even three weeks before the eruption with respect to a measurement made more than one year before (Fig. 4b-d). After the eruption, a temperature increase is visible at the lava flow, but again, there is no significant change in the fumaroles (Fig. 4e). If there was magma or fluids on the move in the months before the eruption in 2011, it seems that the hydrothermal system did not record the change in terms of temperature at the surface. This does not rule out that the hydrothermal system responded to changes in seismicity and ground deformation over shorter time scales of a few months to a few days, as it did in 2007-2008 (Fig. 4b), but were not recorded due to the poor temporal sampling of the available thermal data in 2011. Or perhaps the unrest in the magmatic system did not impact the temperatures of the hydrothermal system at the surface. This might be expected if the magma transfer from depth to the surface was highly localized and happened rapidly, but this partitioning of the hydrothermal system from the rest of the magmatic system calls into question the utility of monitoring surface temperature change as an indicator of magma or fluids on the move at some volcanoes. Unfortunately, there were no gas measurements in the volcano hydrothermal system in the months preceding the eruption and right after it to detect possible changes in the shallow hydrothermal system.

The volcano underwent almost 1 m of uplift right after the end of the 2011-2012 eruption in three discrete pulses during 2012-2018 (Fig. 4a), ongoing as of May 2018, and with very similar spatial footprints [60]. This post-eruptive inflation is not associated with abnormal seismicity [50] or temperature change (Fig. 4b). The fact that the ground deformation followed an exponential trend during the first three years after the eruption [50], as predicted by the magma injection models (section 2b), strongly suggests that the post-eruptive deformation is of magmatic origin. Finite element simulations show that viscoelastic relaxation is of secondary importance with respect to magma injection [60]. Alternatively, inflation after eruption is possible with no recharge for an incompressible magma [57]. While the Cordón Caulle erupted magmas are highly compressible [145], the compressibility of the post-eruptive magma intrusions is not known. The deformation sources are significantly deeper than the inferred depths of the shallow hydrothermal system [50]. All these lines of evidence suggest that the 2012-2018 post-eruptive inflation is most likely of magmatic origin. However, volatile exsolution from depressurization [36] (so-called "first boiling") without significant magma input is another possibility that cannot be excluded in the absence of other datasets and of simulations that can predict the ground deformation temporal evolution.

(g) Aluto, Main Ethiopian Rift (MER) – rift

A recent global compilation suggested that the predictive relationship between deformation and eruption in rift settings was lower than that derived from the global dataset as a whole [124].

Therefore, understanding how to combine multiple datastreams to interpret signals of unrest at volcanic systems within rifts is of key importance. The East African Rift (EAR) is often used as a case study for continental rifting and hosts numerous restless volcanoes [148–150].

Here we focus on Aluto volcano in the MER, as an example of an EAR volcanic system that has been the focus of recent inter-disciplinary study to elucidate the processes driving its unrest. Aluto is a restless silicic volcano/caldera in the MER that last erupted about 400 years ago. The style and volume of recent eruptions suggests that silicic eruptions occur at an average rate of 1 per 1000 years, and that future eruptions of Aluto will involve explosive emplacement of localized pumice cones and effusive obsidian coulees of volumes in the range $1\text{--}100 \times 10^6 \text{ m}^3$ [151]. Aluto has a well-developed hydrothermal system and the complex has been targeted for geothermal development. Diffuse volcanic degassing also takes place at a number of sites across the volcano and it is evident that the pre-existing structures dictate gas and hydrothermal fluid ascent to the surface [152].

Aluto has undergone multiple uplift and subsidence events since 2003 without eruption [149] (Fig. 3d) and understanding the causes of these unrest events has required drawing data together from multiple techniques. Detailed analysis of the InSAR timeseries shows 2 episodes (in 2004 and 2008) of accelerating uplift and edifice-wide inflation, followed initially by rapid subsidence and then slower deflation [153]. The location of the uplift source is roughly centered within the caldera and is constant between 2004 and 2011. Modelling of the uplift finds the best-fit with a spherical point source at a depth of 5.1 km beneath the surface. Deep well observations and magnetotelluric (MT) results place the main geothermal reservoir at a depth of $>2 \text{ km}$ [154,155]. Geochemical modelling of eruptive products suggests that silicic magmas at Aluto are generated and stored at depths of 4–6 km [156]. This suggests that the 5-km inflation source is most likely located between the upper boundary of the magmatic reservoir and base of the geothermal system or within a volatile rich cap in the magma storage zone. At Aluto there is no evidence in the deformation pattern to suggest contracting sources elsewhere around the complex, so it is inferred that inflation was fed from a depth greater than 5 km. As discussed above, deformation data alone do not allow us to unambiguously differentiate between whether the fluid is gas, aqueous fluid, magma, or a combination of these. Hutchison et al. (2016) [153] argue that as most peralkaline volcanoes are considered to have a volatile-rich cap at around 5–6 km depth and that this zone is consistent with the modelled inflation source depth that magmatic fluid injection or intrusions into this cap is the most likely source mechanism for uplift at Aluto.

Further information is contained within the deflation signal at Aluto [153]. The roll-over from uplift to subsidence takes place over a timescale of a few months with analytical source models suggesting that the deflation deformation source is at 3.5 km. This short timescale and shallower depth are strongly suggestive of the migration of magmatic or hydrothermal fluids and degassing with fluids being removed from deep within the geothermal reservoir [157,158]. Gas geochemistry ($\text{CO}_2\text{-}\delta^{13}\text{C}$ [153]) suggests that the magmatic and hydrothermal reservoirs of Aluto are physically connected. Combining the gas and InSAR data with the other constraints on the system described above led Hutchison et al. (2016) [153] to favour a coupled magmatic-hydrothermal process as the mechanism for the Aluto unrest. In their model:

- The uplift is caused by a fresh magmatic fluid pulse or intrusion into a shallow crustal reservoir at 5 km.
- The inflating source region is not well sealed and once pressure builds past a threshold fluids and gas may then leak into the geothermal reservoir and ascend to the surface along fault pathways, resulting in sharp deflation.
- Slow long-term subsidence over the following years may result from continued fluid loss and depressurization of the hydrothermal system consistent with the timescales from numerical simulations of CO_2 -rich magmatic fluid pulses [40].

This coupled model is consistent with the conclusions of Samrock et al. [2015] [155] from MT results who proposed that the apparent lack of a hot extended magma reservoir rules out a pure

magmatic intrusion as the main cause of unrest. It is also consistent with seismic data which has been interpreted to show signals from both the hydrothermal system and the deeper partially crystalline, magmatic mush [159–161]. It is interesting to note, however, that a recently compiled satellite time series implied no temperature change of the fumaroles along Aluto's major faults associated with the deformation cycles between 2004 and 2016 [162].

Rift maturity within the EAR varies, for example, from immature in the Kenyan Rift to intermediate-mature continental rifting in the MER to incipient seafloor spreading in Afar [163]. As well as understanding the signals and implications of unrest in general, key open questions remain about how the symptoms of unrest and its course and consequences (e.g., progression to eruption) change with such variations in rifting processes along the EAR. Drawing together the present literature with future studies combining multiple and extended time series datastreams from restless volcanoes in the Afar, MER and Kenyan rift segments will be key to developing a systematic understanding of volcanic unrest in this region [150,164,165]. Further broader future lessons will be learnt by combining key observations from the EAR with other examples from rift settings such as Iceland [166] and the Taupo volcanic zone [167], New Zealand.

(h) Santorini, Greece – subduction zone

The history of activity at Santorini volcano has been characterized by huge explosive eruptions, sometimes accompanied by caldera formation [168]. Activity between these large-scale events is characterized by intra-caldera edifice construction and lower intensity explosive activity. This is the type of activity that characterizes the current behavior of the system with the last eruption of the intra-caldera Kameni Islands occurring in 1950, 3 decades before the installation of the first instrumental monitoring network [168]. After 60 years of seismic and geodetic quiescence a new period of unrest began in January 2011. Multiple small earthquakes were detected within the caldera, many located along the Kameni line, a fault system thought to have been responsible for the delivery of magma to the surface during previous eruptions [169,170]. Permanent GPS stations and satellite interferometry showed that Santorini was deforming radially and inflating, with parts of northern Nea Kameni rising as much as 15 cm [171]. The rates of seismicity and deformation had returned to baseline levels by September 2012. Modelling of the deformation suggested that over the course of the unrest, two pulses of volume change of 14 - 23 million cubic metres occurred at about 4 km depth (Fig. 3e), beneath the northern caldera [59,172]. Measurements of diffuse CO₂ degassing flux through a small part of the Kameni Islands showed insignificant changes (Fig. 3e) with the onset of unrest [173]. Evidence for the magmatic involvement in the unrest comes from the coincidence of the modelled deformation depth with petrological evidence for the depth of the shallow magma storage zone [174], the H₂/H₂O and CO₂-δ¹³C compositions of the Kameni fumarole gases that indicated an increase in temperature of the system [175] and increases in gas ³He/⁴He ratios indicative of new magma arriving in the system from depth [176]. This evidence does not rule out the hydrothermal system playing a role in driving the unrest however. Radon-CO₂-δ¹³C systematics can even be used to suggest the evolved dacitic nature of the shallow intrusion, again consistent with petrological studies [173,174]. Data from previous Kameni eruptions suggest that this new pulse of magma delivered to the shallow storage zone is a significant fraction of the expected volume of the next eruption should it occur within the next few years [170].

4. Proposed check list for determining cause of volcanic unrest

Based on the review of physical mechanisms and case studies presented in the last two sections, we propose a check-list of criteria (Table 2) that could be consulted during new episodes of unrest to assess the origin of unrest and prioritize new observations that could test hypotheses and help to diagnose the underlying origin and hazards associated with the unrest. Whilst we have focused on subaerial systems, many of the criteria in Table 2 likely apply to submarine magmatic systems. For example, unrest has been identified as having a magmatic origin (as opposed to tectonic

activity) on the Juan de Fuca Ridge on the basis of seismic swarms [177] and hydrothermal fluid samples [106]. However, as on land, there are ambiguities in determining the cause of unrest – the same event on the East Pacific Rise in 1995 can be interpreted as of tectonic (non-magmatic) [178] and magmatic [179] origin.

It is critical that the data collected in Table 2 are available as a time series spanning multiple decades (e.g., Fig. 3). Not only do these time series help define when unrest begins and ends, but the time series reveal trends that are used to infer the origin of unrest [125]. A few of the key observations needed in Table 2 can be made from space (e.g., Fig. 4), albeit with limits on spatial and temporal resolution. However, many key variables at volcanoes (e.g., seismicity, gravity change, CO₂ and other trace gases) cannot be measured from space (or at least easily with current satellites) and so enhanced ground networks are needed. Unfortunately, very few volcanoes have several of the datasets in Table 2 available as a time series and only one or two have the entire suite. Clearly, there is a need to increase the observational record, and so we encourage further discussions to identify the key volcanoes around the world and prioritize the most critical multi-parameter observations from Table 2 to be made. Not all datasets can be collected at all volcanoes – e.g., the fluxes of some gases may not be measurable above background, some volcanoes are open and do not have deformation [124], etc. But where available, as we have shown through the nine examples in section 3, combining geophysics and geochemical data from Table 2 together can be used to develop conceptual models. Yet observations alone will not answer the question of the origin of unrest as magmatic or non-magmatic in many cases – consider the volume of data generated for Campi Flegrei and the debate that still exists about the origin of unrest. Refined interpretations of the origin of unrest may require new datasets (e.g., drilling [115]) and numerical models that can integrate geophysical and geochemical data together [125,180].

The ultimate goal is to use the observations from Table 2 in BET. This is already happening at a few volcanoes that do have multi-decade records of observations (e.g., Fig. 1), but newly identified restless volcanoes (e.g., Aluto) will take time to develop such records. An open question for research is the extent to which we can use the observations used in BET from one volcano and apply them to another [181].

5. Conclusion

A major question in volcano hazard forecasting is understanding the origin of unrest (i.e., magmatic vs. non-magmatic). The importance of this question is growing as we are increasingly able to measure unrest episodes through space and ground based observations. While it is rarely possible to precisely determine the origin of unrest without eruption, schemes like Bayesian Event Trees (BET) are able to incorporate the inherent uncertainty in assessing the cause of unrest into forecasts. We have compiled a set of observations (Table 2) that might be developed in the future to assign probabilities to the origin of unrest, for example via a BET approach. From several case studies it is clear that combining multiple types of observations is critical – no one type of data uniquely pinpoints the origin of unrest. One goal for compiling our list is to help prioritize future observations at volcanoes where the cause of unrest is unclear. But surface observations will not be sufficient as ambiguities remain in interpretation. Further development of numerical models and drilling into these systems to test these models is likely required to advance understanding [120]. We encourage the community to refine and improve upon this list. Further, several restless volcanoes indicate unrest of both magmatic and non-magmatic origin is occurring simultaneously, in combination or in close proximity. Models of a heterogeneous magmatic systems where unrest in different subregions could have different origins is consistent with the TCMS paradigm [1].

Data Accessibility. All data presented here are publicly accessible through published scientific papers.

Authors' Contributions. The paper was conceived by MEP, TM and SM, and all authors contributed to writing and editing the paper.

Competing Interests. The authors declare that they have no competing interests.

Funding. MEP and KR were partly supported by grant NNX16AK87G issued through NASA Science Mission Directorate's Earth Science Division, FJD was supported by a NASA Earth and Space Sciences Fellowship and KR was also supported by the and John Wesley Powell Center for Analysis and Synthesis, funded in part by the U.S. Geological Survey. TAM acknowledges funding from the Natural Environment Research Council via the RiftVolc project (NE/L013932/1, Rift volcanism: past, present, and future) and the Centre for the Observation and Modelling of Earthquakes, Volcanoes, and Tectonics (COMET).

Acknowledgements. This contribution was spurred by discussions at the Royal Society Discussion Meeting on "Magma reservoir architecture and dynamics" and the American Geophysical Union Chapman Conference on "Merging Geophysical, Petrochronological, and Modeling Perspectives of Large Silicic Magma Systems." We thank the organizers and attendees of these meetings as well as Heather Wright for helpful discussions, Mike Poland and an anonymous reviewer for critical comments, and Emily Montgomery-Brown, Will Hutchison, Jaime Farrell, and Valerio Acocella for modified and/or updated figures.

References

1. Sparks RSJ, Cashman KV. Dynamic magma systems: Implications for forecasting volcanic activity. *Elements*. 2017;13(1):35–40.
2. Cashman KV, Sparks RSJ, Blundy JD. Vertically extensive and unstable magmatic systems: a unified view of igneous processes. *Science*. 2017;355(6331):eaag3055.
3. Bachmann O, Bergantz G. The magma reservoirs that feed supereruptions. *Elements*. 2008;4(1):17–21.
4. Cashman KV, Giordano G. Calderas and magma reservoirs. *Journal of Volcanology and Geothermal Research*. 2014;288:28–45.
5. Passarelli L, Brodsky EE. The correlation between run-up and repose times of volcanic eruptions. *Geophysical Journal International*. 2012;188(3):1025–1045.
6. Phillipson G, Sobradelo R, Gottsmann J. Global volcanic unrest in the 21st century: An analysis of the first decade. *Journal of Volcanology and Geothermal Research*. 2013;264:183–196.
7. Larsen J, Neal C, Webley P, Freymueller J, Haney M, McNutt S, et al. Eruption of Alaska volcano breaks historic pattern. *Eos, Transactions American Geophysical Union*. 2009;90(20):173–174.
8. Delgado F, Pritchard ME, Ebmeier S, González P, Lara L. Recent unrest (2002–2015) imaged by space geodesy at the highest risk Chilean volcanoes: Villarrica, Llaima, and Calbuco (Southern Andes). *Journal of Volcanology and Geothermal Research*. 2017;.
9. Rouwet D, Sandri L, Marzocchi W, Gottsmann J, Selva J, Tonini R, et al. Recognizing and tracking volcanic hazards related to non-magmatic unrest: a review. *Journal of Applied Volcanology*. 2014;3(1):17.
10. Moran SC, Newhall C, Roman DC. Failed magmatic eruptions: Late-stage cessation of magma ascent. *Bulletin of Volcanology*. 2011;73(2):115–122.
11. Sobradelo R, Martí J. Bayesian event tree for long-term volcanic hazard assessment: Application to Teide-Pico Viejo stratovolcanoes, Tenerife, Canary Islands. *Journal of Geophysical Research: Solid Earth*. 2010;115(B5).
12. Sobradelo R, Bartolini S, Martí J. HASSET: a probability event tree tool to evaluate future volcanic scenarios using Bayesian inference. *Bulletin of Volcanology*. 2014;76(1):770.
13. Sandri L, Tonini R, Rouwet D, Constantinescu R, Mendoza-Rosas AT, Andrade D, et al. The need to quantify hazard related to non-magmatic unrest: from BET_EF to BET_UNREST.

- Advances in Volcanology. 2017;.
14. Dzurisin D, Wicks CW, Poland MP.
History of surface displacements at the Yellowstone Caldera, Wyoming, from leveling surveys and InSAR observations, 1923-2008.
US Geological Survey; 2012.
 15. Acocella V, Di Lorenzo R, Newhall C, Scandone R.
An overview of recent (1988 to 2014) caldera unrest: Knowledge and perspectives.
Reviews of Geophysics. 2015;53(3):896–955.
 16. Gottsmann J, Folch A, Rymer H.
Unrest at Campi Flegrei: A contribution to the magmatic versus hydrothermal debate from inverse and finite element modeling.
Journal of Geophysical Research: Solid Earth. 2006;111(B7).
 17. Fournier T, Pritchard ME, Riddick SN.
The frequency, duration, and magnitude of subaerial volcano deformation events: New results from Latin America and a global synthesis.
Geochem, Geophys, Geosys. 2010;11.
 18. Jay JA, Welch M, Pritchard ME, Mares PJ, Mnich ME, Melkonian AK, et al.
Volcanic hotspots of the central and southern Andes as seen from space by ASTER and MODVOLC between the years 2000-2010.
In: Pyle D, Mather TA, Biggs J, editors. Remote Sensing of Volcanoes and Volcanic Processes: Integrating Observation and Modelling. vol. 380. London: Geological Society of London; 2013. p. 161–185.
 19. Brown S, Loughlin S, Sparks R, Vye-Brown C. Global volcanic hazards and risk: Technical background paper for the global assessment report on disaster risk reduction 2015; 2015.
Available from: <http://www.preventionweb.net/english/hyogo/gar/2015/en/bgddocs/GVM,%202014b.pdf>.
 20. Wicks CW, Thatcher W, Dzurisin D, Svarc J.
Uplift, thermal unrest and magma intrusion at Yellowstone caldera.
Nature. 2006;440(7080):72.
 21. Carbone D, Poland MP, Diamant M, Greco F.
The added value of time-variable microgravimetry to the understanding of how volcanoes work.
Earth-Science Reviews. 2017;169:146–179.
 22. Battaglia M, Troise C, Obrizzo F, Pingue F, De Natale G.
Evidence for fluid migration as the source of deformation at Campi Flegrei caldera (Italy).
Geophysical Research Letters. 2006;33(1).
 23. Miller C, Le Mével H, Currenti G, Williams-Jones G, Tikoff B.
Microgravity changes at the Laguna del Maule volcanic field: Magma-induced stress changes facilitate mass addition.
Journal of Geophysical Research: Solid Earth. 2017;122(4):3179–3196.
 24. Battaglia M, Roberts C, Segall P.
Magma intrusion beneath Long Valley caldera confirmed by temporal changes in gravity.
Science. 1999;285(5436):2119–2122.
 25. Tizzani P, Battaglia M, Zeni G, Atzori S, Berardino P, Lanari R.
Uplift and magma intrusion at Long Valley caldera from InSAR and gravity measurements.
Geology. 2009;37(1):63–66.
 26. Tizzani P, Battaglia M, Castaldo R, Pepe A, Zeni G, Lanari R.
Magma and fluid migration at Yellowstone Caldera in the last three decades inferred from InSAR, leveling, and gravity measurements.
Journal of Geophysical Research: Solid Earth. 2015;120(4):2627–2647.
 27. Poland MP, Carbone D.
Insights into shallow magmatic processes at Kīlauea Volcano, HawaiĒi, from a multiyear continuous gravity time series.
Journal of Geophysical Research: Solid Earth. 2016;121(7):5477–5492.
 28. Bagnardi M, Poland MP, Carbone D, Baker S, Battaglia M, Amelung F.
Gravity changes and deformation at Kīlauea Volcano, Hawaii, associated with summit eruptive activity, 2009–2012.
Journal of Geophysical Research: Solid Earth. 2014;119(9):7288–7305.

29. Lloyd R, Biggs J, Birhanu Y.
(Sustained uplift at a continental rift caldera (abstract #496).
In: IAVCEI Scientific Assembly, Portland, Oregon; 2017. .
30. Johnson DJ, Eggers AA, Bagnardi M, Battaglia M, Poland MP, Miklius A.
Shallow magma accumulation at Kilauea Volcano, Hawai   i, revealed by microgravity surveys.
Geology. 2010;38(12):1139–1142.
31. Greco F, Currenti G, Palano M, Pepe A, Pepe S.
Evidence of a shallow persistent magmatic reservoir from joint inversion of gravity and ground deformation data: The 25–26 October 2013 Etna lava fountaining event.
Geophysical Research Letters. 2016;43(7):3246–3253.
32. Hildreth W.
Fluid-driven uplift at Long Valley Caldera, California: Geologic perspectives.
Journal of Volcanology and Geothermal Research. 2017;341:269–286.
33. Hautmann S, Gottsmann J.
Ground Deformation and Gravity Changes of the Kos-Nisyros Volcanic System Between 1995 and 2008.
In: Nisyros Volcano. Springer; 2018. p. 303–319.
34. Carbone D, Zuccarello L, Saccorotti G, Greco F.
Analysis of simultaneous gravity and tremor anomalies observed during the 2002–2003 Etna eruption.
Earth and Planetary Science Letters. 2006;245(3–4):616–629.
35. Middlemiss R, Samarelli A, Paul D, Hough J, Rowan S, Hammond G.
Measurement of the Earth tides with a MEMS gravimeter.
Nature. 2016;531(7596):614.
36. Tait S, Jaupart C, Vergn  lle S.
Pressure, gas content and eruption periodicity of a shallow, crystallising magma chamber.
Earth and Planetary Science Letters. 1989;92(1):107–123.
37. Pritchard ME, Gregg PM.
Geophysical evidence for silicic crustal melt in the continents: where, what kind, and how much?
Elements. 2016;12(2):121–127.
38. Newhall CG, Dzurisin D.
Historical unrest at the large calderas of the world.
1855. Department of the Interior, US Geological Survey; 1988.
39. Gottsmann J, Blundy J, Henderson S, Pritchard M, Sparks R.
Thermomechanical modeling of the Altiplano-Puna deformation anomaly: Multiparameter insights into magma mush reorganization.
Geosphere. 2017;13(4):1042–1065.
40. Chiodini G, Caliro S, De Martino P, Avino R, Gherardi F.
Early signals of new volcanic unrest at Campi Flegrei caldera? Insights from geochemical data and physical simulations.
Geology. 2012;40(10):943–946.
41. Kaizuka S.
Coastal evolution at a rapidly uplifting volcanic island: Iwo-Jima, western Pacific Ocean.
Quaternary International. 1992;15:7–16.
42. Singer BS, Le M  vel H, Licciardi JM, C  rdova L, Tikoff B, Garibaldi N, et al.
Geomorphic expression of rapid Holocene silicic magma reservoir growth beneath Laguna del Maule, Chile.
Science advances. 2018;4(6):eaat1513.
43. Sion B, Axen G, Phillips F, van Wijk J.
Geomorphic Evidence for Episodic Inflation Above the Socorro Magma Body: Timescales and Mechanisms Related to Surface Uplift.
In: New Mexico Geological Society Annual Spring Meeting; 2018. .
44. Passaro S, Tamburrino S, Vallef  uoco M, Tassi F, Vaselli O, Giannini L, et al.
Seafloor doming driven by degassing processes unveils sprouting volcanism in coastal areas.
Scientific reports. 2016;6:22448.
45. Pierce KL, Cannon KP, Meyer GA, Trebesch MJ, Watts RD.

- Post-glacial inflation-deflation cycles, tilting, and faulting in the Yellowstone caldera based on Yellowstone Lake shorelines.
US Geological Survey; 2002.
46. Finnegan NJ, Pritchard ME.
Magnitude and duration of surface uplift above the Socorro magma body.
Geology. 2009;37(3):231–234.
 47. Perkins JP, Finnegan NJ, Henderson ST, Rittenour TM.
Topographic constraints on magma accumulation below the actively uplifting Uturuncu and Lazufre volcanic centers in the Central Andes.
Geosphere. 2016;12(4):1078–1096.
 48. Le Mével H, Feigl KL, Córdova L, DeMets C, Lundgren P.
Evolution of unrest at Laguna del Maule volcanic field (Chile) from InSAR and GPS measurements, 2003 to 2014.
Geophysical Research Letters. 2015;42(16):6590–6598.
 49. Le Mével H, Gregg PM, Feigl KL.
Magma injection into a long-lived reservoir to explain geodetically measured uplift: Application to the 2007–2014 unrest episode at Laguna del Maule volcanic field, Chile.
Journal of Geophysical Research: Solid Earth. 2016;121(8):6092–6108.
 50. Delgado F, Pritchard ME, Basualto D, Lazo J, Córdova L, Lara LE.
Rapid reinflation following the 2011–2012 rhyodacite eruption at Cordón Caulle volcano (Southern Andes) imaged by InSAR: Evidence for magma reservoir refill.
Geophysical Research Letters. 2016;43(18):9552–9562.
 51. Henderson ST, Delgado F, Elliott J, Pritchard ME, Lundgren PR.
Decelerating uplift at Lazufre volcanic center, central Andes, from A.D. 2010 to 2016, and implications for geodetic models.
Geosphere. 2017;in press.
 52. Lengliné O, Marsan D, Got JL, Pinel V, Ferrazzini V, Okubo P.
Seismicity and deformation induced by magma accumulation at three basaltic volcanoes.
Journal of Geophysical Research: Solid Earth. 2008;113(B12).
 53. Lu Z, Masterlark T, Dzurisin D, Rykhus R, C Wicks J.
Magma supply dynamics at Westdahl volcano, Alaska, modeled from satellite radar interferometry.
J Geophys Res. 2003;108(B7).
 54. Lu Z, Dzurisin D, Biggs J, Wicks C, McNutt S.
Ground surface deformation patterns, magma supply, and magma storage at Okmok volcano, Alaska, from InSAR analysis: 1. Intereruption deformation, 1997–2008.
Journal of Geophysical Research: Solid Earth. 2010;115(B5).
 55. Reverso T, Vandemeulebrouck J, Jouanne F, Pinel V, Villemin T, Sturkell E, et al.
A two-magma chamber model as a source of deformation at Grímsvötn Volcano, Iceland.
Journal of Geophysical Research: Solid Earth. 2014;119(6):4666–4683.
 56. Bagnardi M, Amelung F.
Space-geodetic evidence for multiple magma reservoirs and subvolcanic lateral intrusions at Fernandina Volcano, Galápagos Islands.
Journal of Geophysical Research: Solid Earth. 2012;117(B10).
 57. Segall P.
Repressurization following eruption from a magma chamber with a viscoelastic aureole.
Journal of Geophysical Research: Solid Earth. 2016;121(12):8501–8522.
 58. Newman AV, Dixon TH, Gourmelen N.
A four-dimensional viscoelastic model for deformation of the Long Valley caldera, California, between 1995 and 2000.
J Volc Geotherm Res. 2006;150:244–269.
 59. Parks MM, Moore JD, Papanikolaou X, Biggs J, Mather TA, Pyle DM, et al.
From quiescence to unrest: 20 years of satellite geodetic measurements at Santorini volcano, Greece.
Journal of Geophysical Research: Solid Earth. 2015;120(2):1309–1328.
 60. Delgado FJ.
Magma Storage, Transport and Eruption Dynamics in the Southern Andean Volcanic Zone Imaged with InSAR Geodesy.

- Ph.D. Thesis, Cornell University; 2018.
61. Hurwitz S, Christiansen LB, Hsieh PA.
Hydrothermal fluid flow and deformation in large calderas: Inferences from numerical simulations.
Journal of Geophysical Research: Solid Earth. 2007;112(B2).
 62. Hutnak M, Hurwitz S, Ingebritsen S, Hsieh P.
Numerical models of caldera deformation: Effects of multiphase and multicomponent hydrothermal fluid flow.
Journal of Geophysical Research: Solid Earth. 2009;114(B4).
 63. Fournier N, Chardot L.
Understanding volcano hydrothermal unrest from geodetic observations: Insights from numerical modeling and application to White Island volcano, New Zealand.
Journal of Geophysical Research: Solid Earth. 2012;117(B11).
 64. Menyailov I, Nikitina L, Shapar V, Pilipenko V.
Temperature increase and chemical change of fumarolic gases at Momotombo volcano, Nicaragua, in 1982–1985: are these indicators of a possible eruption?
Journal of Geophysical Research: Solid Earth. 1986;91(B12):12199–12214.
 65. Shinohara H, Giggenbach WF, Kazahaya K, Hedenquist JW.
Geochemistry of volcanic gases and hot springs of Satsuma-Iwojima, Japan: Following Matsuo.
Geochemical Journal. 1993;27(4-5):271–285.
 66. Shinohara H, Kazahaya K, Saito G, Matsushima N, Kawanabe Y.
Degassing activity from Iwodake rhyolitic cone, Satsuma-Iwojima volcano, Japan: Formation of a new degassing vent, 1990–1999.
Earth, planets and space. 2002;54(3):175–185.
 67. Taran YA, Hedenquist J, Korzhinsky M, Tkachenko S, Shmulovich K.
Geochemistry of magmatic gases from Kudryavy volcano, Iturup, Kuril Islands.
Geochimica et Cosmochimica Acta. 1995;59(9):1749–1761.
 68. Global Volcanism Program. *Volcanoes of the World*, v. 4.6.0.; 2017.
[Date accessed: 20 June 2017].
Smithsonian Institution, Venzke, E. (ed.).
 69. Sawyer G, Salerno G, Le Blond J, Martin R, Spampinato L, Roberts T, et al.
Gas and aerosol emissions from Villarrica volcano, Chile.
Journal of Volcanology and Geothermal Research. 2011;203(1-2):62–75.
 70. Kern C, Masias P, Apaza F, Reath KA, Platt U.
Remote measurement of high preeruptive water vapor emissions at Sabancaya volcano by passive differential optical absorption spectroscopy.
Journal of Geophysical Research: Solid Earth. 2017;122(5):3540–3564.
 71. Ebmeier SK, Elliott JR, Nocquet JM, Biggs J, Mothes P, Jarrín P, et al.
Shallow earthquake inhibits unrest near Chiles–Cerro Negro volcanoes, Ecuador–Colombian border.
Earth and Planetary Science Letters. 2016;450:283–291.
 72. Jay JA, Delgado FJ, Torres JL, Pritchard ME, Macedo O, Aguilar V.
Deformation and seismicity near Sabancaya volcano, southern Peru, from 2002 to 2015.
Geophysical Research Letters. 2015;42(8):2780–2788.
 73. Benoit JP, McNutt SR.
Global volcanic earthquake swarm database and preliminary analysis of volcanic earthquake swarm duration.
Annali di Geofisica. 1996;39(2):221.
 74. McNutt SR.
Seismic monitoring and eruption forecasting of volcanoes: a review of the state-of-the-art and case histories.
In: *Monitoring and mitigation of volcano hazards*. Springer; 1996. p. 99–146.
 75. McNutt SR.
Volcanic seismology.
Annu Rev Earth Planet Sci. 2005;32:461–491.
 76. Power JA, Lahr JC, Page RA, Chouet BA, Stephens CD, Harlow DH, et al.
Seismic evolution of the 1989–1990 eruption sequence of Redoubt Volcano, Alaska.

- Journal of Volcanology and Geothermal Research. 1994;62(1-4):69–94.
77. Leet RC.
Saturated and subcooled hydrothermal boiling in groundwater flow channels as a source of harmonic tremor.
Journal of Geophysical Research: Solid Earth. 1988;93(B5):4835–4849.
 78. McNutt SR.
Volcanic tremor.
Encyclopedia of earth system science. 1992;4:417–425.
 79. Jacobs KM, McNutt SR.
Using seismic b-values to interpret seismicity rates and physical processes during the preeruptive earthquake swarm at Augustine Volcano 2005–2006.
US Geological Survey Professional Paper 1769. 2010;p. 59–83.
 80. Passarelli L, Heryandoko N, Cesca S, Rivalta E, Rohadi S, Dahm T, et al.
Magmatic or not magmatic? The 2015–2016 seismic swarm at the long-dormant Jailolo volcano, West Halmahera, Indonesia.
Frontiers in Earth Science. 2018;6:79.
 81. Aki K, Koyanagi R.
Deep volcanic tremor and magma ascent mechanism under Kilauea, Hawaii.
Journal of Geophysical Research: Solid Earth. 1981;86(B8):7095–7109.
 82. White RA.
Precursory deep long-period earthquakes at Mount Pinatubo: Spatio-temporal link to a basalt trigger.
Fire and mud: Eruptions and lahars of Mount Pinatubo, Philippines. 1996;p. 307–328.
 83. Power JA, Jolly A, Page R, McNutt S.
Seismicity and forecasting of the 1992 eruptions of Crater Peak vent, Mount Spurr Volcano, Alaska: an overview.
The 1992 Eruptions of Crater Peak Vent, Mount Spurr Volcano, Alaska. 1995;2139:149–159.
 84. Hill DP, Prejean S.
Magmatic unrest beneath Mammoth Mountain, California.
Journal of Volcanology and Geothermal Research. 2005;146(4):257–283.
 85. Neuberg J, Luckett R, Ripepe M, Braun T.
Highlights from a seismic broadband array on Stromboli volcano.
Geophysical Research Letters. 1994;21(9):749–752.
 86. Kawakatsu H, Kaneshima S, Matsubayashi H, Ohminato T, Sudo Y, Tsutsui T, et al.
Aso94: Aso seismic observation with broadband instruments.
Journal of Volcanology and Geothermal Research. 2000;101(1-2):129–154.
 87. Klein FW, Koyanagi RY, Nakata JS, Tanigawa WR.
The seismicity of Kilauea's magma system.
US Geol Surv Prof Pap. 1987;1350(2):1019–1185.
 88. Chiodini G, Paonita A, Aiuppa A, Costa A, Caliro S, De Martino P, et al.
Magmas near the critical degassing pressure drive volcanic unrest towards a critical state.
Nature communications. 2016;7:13712.
 89. Lowenstern JB, Bergfeld D, Evans WC, Hunt AG.
Origins of geothermal gases at Yellowstone.
Journal of Volcanology and Geothermal Research. 2015;302:87–101.
 90. Daag AS, Tubianosa BS, Newhall C, Tungol N, Javier D, Dolan M, et al.
Monitoring sulfur dioxide emission at Mount Pinatubo.
In: Newhall CG, PUNONGBAYAN AS, editors. Fire and Mud: eruptions and lahars of Mount Pinatubo, Philippines. University of Washington Press Seattle, WA; 1996. p. 409–414.
 91. De Moor J, Aiuppa A, Pacheco J, Avaré G, Kern C, Liuzzo M, et al.
Short-period volcanic gas precursors to phreatic eruptions: Insights from Poás Volcano, Costa Rica.
Earth and Planetary Science Letters. 2016;442:218–227.
 92. Aiuppa A, Bitetto M, Francofonte V, Velasquez G, Bucarey Parra C, Giudice G, et al.
A CO₂-gas precursor to the March 2015 Villarrica volcano eruption.
Geochemistry, Geophysics, Geosystems. 2017;.
 93. Aiuppa A, Moretti R, Federico C, Giudice G, Gurrieri S, Liuzzo M, et al.
Forecasting Etna eruptions by real-time observation of volcanic gas composition.

- Geology. 2007;35(12):1115–1118.
94. Aiuppa A, Federico C, Giudice G, Giuffrida G, Guida R, Gurrieri S, et al.
The 2007 eruption of Stromboli volcano: insights from real-time measurement of the volcanic gas plume CO₂/SO₂ ratio.
Journal of Volcanology and Geothermal Research. 2009;182(3-4):221–230.
 95. Surono PJ, Pallister J, Boichu M, Buongiorno MF, Budisantoso A, Costa F, et al.
The 2010 explosive eruption of Java's Merapi volcano – a 100-year event.
Journal of Volcanology and Geothermal Research. 2012;241:121–135.
 96. Lewicki JL, Hilley GE.
Multi-scale observations of the variability of magmatic CO₂ emissions, Mammoth Mountain, CA, USA.
Journal of Volcanology and Geothermal Research. 2014;284:1–15.
 97. Macpherson C, Matthey D.
Carbon isotope variations of CO₂ in Central Lau Basin basalts and ferrobasalts.
Earth and planetary science letters. 1994;121(3-4):263–276.
 98. Ballentine CJ, Burgess R, Marty B.
Tracing fluid origin, transport and interaction in the crust.
Reviews in mineralogy and geochemistry. 2002;47(1):539–614.
 99. Chiodini G, Marini L.
Hydrothermal gas equilibria: the H₂O – H₂ – CO₂ – CO – CH₄ system.
Geochimica et Cosmochimica Acta. 1998;62(15):2673–2687.
 100. Lowenstern JB, Janik CJ.
The origins of reservoir liquids and vapors from The Geysers geothermal field, California (USA).
Volcanic, Geothermal and Ore-forming Fluids: Rulers and Witnesses of Processes within the Earth: Soc of Econ Geologists Special Pub. 2003;10:181–195.
 101. Soosalu H, Einarsson P.
Seismic constraints on magma chambers at Hekla and Torfajökull volcanoes, Iceland.
Bulletin of Volcanology. 2004;66(3):276–286.
 102. Fournier R.
Chemical geothermometers and mixing models for geothermal systems.
Geothermics. 1977;5(1-4):41–50.
 103. Varekamp JC.
The chemical composition and evolution of volcanic lakes.
In: volcanic lakes. Springer; 2015. p. 93–123.
 104. Taran Y, Rouwet D, Inguaggiato S, Aiuppa A.
Major and trace element geochemistry of neutral and acidic thermal springs at El Chichón volcano, Mexico: implications for monitoring of the volcanic activity.
Journal of Volcanology and Geothermal Research. 2008;178(2):224–236.
 105. Maussen K, Villacorte E, Rebadulla RR, Maximo RP, Debaille V, Bornas MA, et al.
Geochemical characterisation of Taal volcano-hydrothermal system and temporal evolution during continued phases of unrest (1991–2017).
Journal of volcanology and geothermal research. 2018;352:38–54.
 106. Lilley MD, Butterfield DA, Lupton JE, Olson EJ.
Magmatic events can produce rapid changes in hydrothermal vent chemistry.
Nature. 2003;422(6934):878.
 107. Lowenstern JB, Hurwitz S.
Monitoring a supervolcano in repose: Heat and volatile flux at the Yellowstone Caldera.
Elements. 2008;4(1):35–40.
 108. Chiodini G, Vandemeulebrouck J, Caliro S, D'Auria L, De Martino P, Mangiacapra A, et al.
Evidence of thermal-driven processes triggering the 2005–2014 unrest at Campi Flegrei caldera.
Earth and Planetary Science Letters. 2015;414:58–67.
 109. Linde AT, Sacks S, Hidayat D, Voight B, Clarke A, Elsworth D, et al.
Vulcanian explosion at Soufrière Hills Volcano, Montserrat on March 2004 as revealed by strain data.
Geophysical Research Letters. 2010;37(19).
 110. Bonaccorso A, Currenti G, Linde A, Sacks S.

- New data from borehole strainmeters to infer lava fountain sources (Etna 2011–2012). *Geophysical Research Letters*. 2013;40(14):3579–3584.
111. Eichelberger JC, Uto K.
Active volcanic systems.
In: *Continental Scientific Drilling*. Springer; 2007. p. 213–234.
 112. Eichelberger JC, Lysne PC, Younker LW.
Research drilling at Inyo Domes, Long Valley Caldera, California.
Eos, Transactions American Geophysical Union. 1984;65(39):721–725.
 113. Elders WA, Sass JH.
The Salton Sea scientific drilling project.
Journal of Geophysical Research: Solid Earth. 1988;93(B11):12953–12968.
 114. Saito S, Sakuma S, Uchida T.
Drilling procedures, techniques and test results for a 3.7 km deep, 500 C exploration well, Kakkonda, Japan.
Geothermics. 1998;27(5-6):573–590.
 115. Carlino S, Kilburn CR, Tramelli A, Troise C, Somma R, De Natale G.
Tectonic stress and renewed uplift at Campi Flegrei caldera, southern Italy: new insights from caldera drilling.
Earth and Planetary Science Letters. 2015;420:23–29.
 116. Sorey ML, McConnell VS, Roeloffs E.
Summary of recent research in Long Valley caldera, California.
Journal of volcanology and geothermal research. 2003;127(3-4):165–173.
 117. Teplow W, Marsh B, Hulen J, Spielman P, Kaleikini M, Fitch D, et al.
Dacite melt at the Puna geothermal venture wellfield, Big Island of Hawaii.
Geothermal Resources Council Transactions. 2009;33:989–994.
 118. Elders W, Friðleifsson G, Albertsson A.
Drilling into magma and the implications of the Iceland Deep Drilling Project (IDDP) for high-temperature geothermal systems worldwide.
Geothermics. 2014;49:111–118.
 119. Mbia P, Mortensen A, Oskarsson N, Hardarson B.
Sub-surface geology, petrology and hydrothermal alteration of the Menengai geothermal field, Kenya: case study of wells MW-02, MW-04, MW-06 and MW-07.
In: *Proceedings World Geothermal Congress*; 2015. p. 20.
 120. Lowenstern JB, Sisson TW, Hurwitz S.
Probing Magma Reservoirs to Improve Volcano Forecasts.
EOS-Earth & Space Science News. 2017;.
 121. National Academies of Sciences E, Medicine.
Volcanic eruptions and their repose, unrest, precursors, and timing.
National Academies Press; 2017.
 122. Till CB, Pritchard M, Miller CA, Brugman KK, Ryan-Davis J.
Super-volcanic investigations.
Nature Geoscience. 2018;11(4):227.
 123. Dobson P, Asanuma H, Huenges E, Poletto F, Reinsch T, Sanjuan B.
Supercritical geothermal systems-a review of past studies and ongoing research activities.
In: *42nd Workshop on Geothermal Reservoir Engineering*; 2017. .
 124. Biggs J, Ebmeier S, Aspinall W, Lu Z, Pritchard M, Sparks R, et al.
Global link between deformation and volcanic eruption quantified by satellite imagery.
Nature communications. 2014;5.
 125. Moretti R, De Natale G, Troise C.
A geochemical and geophysical reappraisal to the significance of the recent unrest at Campi Flegrei caldera (Southern Italy).
Geochemistry, Geophysics, Geosystems. 2017;18(3):1244–1269.
 126. Kilburn CR, De Natale G, Carlino S.
Progressive approach to eruption at Campi Flegrei caldera in southern Italy.
Nature communications. 2017;8:15312.
 127. Chiodini G, Todesco M, Caliro S, Del Gaudio C, Macedonio G, Russo M.
Magma degassing as a trigger of bradyseismic events: The case of Phlegrean Fields (Italy).
Geophysical Research Letters. 2003;30(8).

128. Caliro S, Chiodini G, Paonita A.
Geochemical evidences of magma dynamics at Campi Flegrei (Italy).
Geochimica et cosmochimica acta. 2014;132:1–15.
129. Morhange C, Marriner N, Laborel J, Todesco M, Oberlin C.
Rapid sea-level movements and noneruptive crustal deformations in the Phlegrean Fields caldera, Italy.
Geology. 2006;34(2):93–96.
130. Bellucci F, Woo J, Kilburn CR, Rolandi G.
Ground deformation at Campi Flegrei, Italy: implications for hazard assessment.
Geological Society, London, Special Publications. 2006;269(1):141–157.
131. Farrell J, Smith RB, Husen S, Diehl T.
Tomography from 26 years of seismicity revealing that the spatial extent of the Yellowstone crustal magma reservoir extends well beyond the Yellowstone caldera.
Geophysical Research Letters. 2014;41(9):3068–3073.
132. Huang HH, Lin FC, Schmandt B, Farrell J, Smith RB, Tsai VC.
The Yellowstone magmatic system from the mantle plume to the upper crust.
Science. 2015;348(6236):773–776.
133. Hurwitz S, Lowenstern JB.
Dynamics of the Yellowstone hydrothermal system.
Reviews of Geophysics. 2014;52(3):375–411.
134. Pritchard M, de Silva S, Michelfelder G, Zandt G, McNutt S, Gottsmann J, et al.
Synthesis: PLUTONS: Investigating the relationship between pluton growth and volcanism in the Central Andes.
Geosphere. 2018;.
135. Froger JL, Rémy D, Bonvalot S, Legrand D.
Two scales of inflation at Lastarria-Cordon del Azufre volcanic complex, central Andes, revealed from ASAR-ENVISAT interferometric data.
Earth and Planetary Science Letters. 2007;255(1-2):148–163.
136. Aguilera F, Tassi F, Darrah T, Moune S, Vaselli O.
Geochemical model of a magmatic–hydrothermal system at the Lastarria volcano, northern Chile.
Bulletin of volcanology. 2012;74(1):119–134.
137. Lopez T, Aguilera F, Tassi F, de Moor JM, Bobrowski N, Aiuppa A, et al.
New insights into the magmatic–hydrothermal system and volatile budget of Lastarria volcano, Chile: Integrated results from the 2014 IAVCEI CCGV 12th Volcanic Gas Workshop.
Geosphere. 2018;14(3):983–1007.
138. Pritchard M, Simons M.
An InSAR-based survey of volcanic deformation in the central Andes.
Geochemistry, Geophysics, Geosystems. 2004;5(2).
139. Fialko Y, Pearse J.
Sombbrero uplift above the Altiplano-Puna magma body: Evidence of a ballooning mid-crustal diapir.
Science. 2012;338(6104):250–252.
140. Jay JA, Pritchard ME, West ME, Christensen D, Haney M, Minaya E, et al.
Shallow seismicity, triggered seismicity, and ambient noise tomography at the long-dormant Uturuncu Volcano, Bolivia.
Bulletin of Volcanology. 2012;74(4):817–837.
141. Lau N, Tymofyeyeva E, Fialko Y.
Variations in the long-term uplift rate due to the Altiplano–Puna magma body observed with Sentinel-1 interferometry.
Earth and Planetary Science Letters. 2018;491:43–47.
142. Singer BS, Andersen NL, Le Mével H, Feigl KL, DeMets C, Tikoff B, et al.
Dynamics of a large, restless, rhyolitic magma system at Laguna del Maule, southern Andes, Chile.
GSA Today. 2014;24(12):4–10.
143. Cordell D, Unsworth MJ, Díaz D.
Imaging the Laguna del Maule Volcanic Field, central Chile using magnetotellurics: Evidence for crustal melt regions laterally-offset from surface vents and lava flows.

- Earth and Planetary Science Letters. 2018;488:168–180.
144. Castro JM, Schipper CI, Mueller SP, Militzer A, Amigo A, Parejas CS, et al.
Storage and eruption of near-liquidus rhyolite magma at Cordón Caulle, Chile.
Bulletin of Volcanology. 2013;75(4):702.
 145. Jay J, Costa F, Pritchard M, Lara L, Singer B, Herrin J.
Locating magma reservoirs using InSAR and petrology before and during the 2011–2012 Cordón Caulle silicic eruption.
Earth and Planetary Science Letters. 2014;395:254–266.
 146. Sepúlveda F, Dorsch K, Lahsen A, Bender S, Palacios C.
Chemical and isotopic composition of geothermal discharges from the Puyehue-Cordón Caulle area (40.5 S), Southern Chile.
geothermics. 2004;33(5):655–673.
 147. Wendt A, Tassara A, Báez JC, Basualto D, Lara LE, García F.
Possible structural control on the 2011 eruption of Puyehue-Cordón Caulle Volcanic Complex (southern Chile) determined by InSAR, GPS and seismicity.
Geophysical Journal International. 2017;208(1):134–147.
 148. Grandin R, Socquet A, Doin MP, Jacques E, de Chabaliér JB, King G.
Transient rift opening in response to multiple dike injections in the Manda Hararo rift (Afar, Ethiopia) imaged by time-dependent elastic inversion of interferometric synthetic aperture radar data.
Journal of Geophysical Research: Solid Earth. 2010;115(B9).
 149. Biggs J, Bastow I, Keir D, Lewi E.
Pulses of deformation reveal frequently recurring shallow magmatic activity beneath the Main Ethiopian Rift.
Geochemistry, Geophysics, Geosystems. 2011;12(9).
 150. Hamlyn JE, Keir D, Wright TJ, Neuberg JW, Goitom B, Hammond JO, et al.
Seismicity and subsidence following the 2011 Nabro eruption, Eritrea: Insights into the plumbing system of an off-rift volcano.
Journal of Geophysical Research: Solid Earth. 2014;119(11):8267–8282.
 151. Hutchison W, Pyle DM, Mather TA, Yirgu G, Biggs J, Cohen BE, et al.
The eruptive history and magmatic evolution of Aluto volcano: new insights into silicic peralkaline volcanism in the Ethiopian rift.
Journal of Volcanology and Geothermal Research. 2016;328:9–33.
 152. Hutchison W, Mather TA, Pyle DM, Biggs J, Yirgu G.
Structural controls on fluid pathways in an active rift system: A case study of the Aluto volcanic complex.
Geosphere. 2015;11(3):542–562.
 153. Hutchison W, Biggs J, Mather TA, Pyle DM, Lewi E, Yirgu G, et al.
Causes of unrest at silicic calderas in the East African Rift: New constraints from InSAR and soil-gas chemistry at Aluto volcano, Ethiopia.
Geochemistry, Geophysics, Geosystems. 2016;17(8):3008–3030.
 154. Teklemariam M, Battaglia S, Gianelli G, Ruggieri G.
Hydrothermal alteration in the Aluto-Langano geothermal field, Ethiopia.
Geothermics. 1996;25(6):679–702.
 155. Samrock F, Kuvshinov A, Bakker J, Jackson A, Fisseha S.
3-D analysis and interpretation of magnetotelluric data from the Aluto-Langano geothermal field, Ethiopia.
Geophysical Journal International. 2015;202(3):1923–1948.
 156. Gleeson ML, Stock MJ, Pyle DM, Mather TA, Hutchison W, Yirgu G, et al.
Constraining magma storage conditions at a restless volcano in the Main Ethiopian Rift using phase equilibria models.
Journal of Volcanology and Geothermal Research. 2017;337:44–61.
 157. Wauthier C, Cayol V, Poland M, Kervyn F, Oreye N, Hooper A, et al.
Nyamulagira's magma plumbing system inferred from 15 years of InSAR.
Geological Society, London, Special Publications. 2013;380(1):39–65.
 158. Caricchi L, Biggs J, Annen C, Ebmeier S.
The influence of cooling, crystallisation and re-melting on the interpretation of geodetic signals in volcanic systems.

- Earth and Planetary Science Letters. 2014;388:166–174.
159. Wilks M, Kendall JM, Nowacki A, Biggs J, Wookey J, Birhanu Y, et al.
Seismicity associated with magmatism, faulting and hydrothermal circulation at Aluto Volcano, Main Ethiopian Rift.
Journal of Volcanology and Geothermal Research. 2017;340:52–67.
 160. Nowacki A, Wilks M, Kendall JM, Biggs J, Ayele A.
Characterising hydrothermal fluid pathways beneath Aluto volcano, Main Ethiopian Rift, using shear wave splitting.
Journal of Volcanology and Geothermal Research. 2018;.
 161. Birhanu Y, Wilks M, Biggs J, Kendall JM, Ayele A, Lewi E.
Seasonal patterns of seismicity and deformation at the Alutu geothermal reservoir, Ethiopia, induced by hydrological loading.
Journal of Volcanology and Geothermal Research. 2018;356:175–182.
 162. Braddock M, Biggs J, Watson IM, Hutchison W, Pyle DM, Mather TA.
Satellite observations of fumarole activity at Aluto volcano, Ethiopia: Implications for geothermal monitoring and volcanic hazard.
Journal of Volcanology and Geothermal Research. 2017;341:70–83.
 163. Ebinger C.
Continental break-up: the East African perspective.
Astronomy & Geophysics. 2005;46(2):2–16.
 164. Lloyd R, Biggs J, Birhanu Y, Wilks M, Gottsmann J, Kendall JM, et al.
Sustained Uplift at a Continental Rift Caldera.
Journal of Geophysical Research: Solid Earth. 2018;.
 165. Biggs J, Robertson E, Cashman K.
The lateral extent of volcanic interactions during unrest and eruption.
Nature Geoscience. 2016;9(4):308.
 166. Sigmundsson F, Hooper A, Hreinsdóttir S, Vogfjörð KS, Ófeigsson BG, Heimisson ER, et al.
Segmented lateral dyke growth in a rifting event at Bárðarbunga volcanic system, Iceland.
Nature. 2015;517(7533):191.
 167. Bibby H, Caldwell T, Davey F, Webb T.
Geophysical evidence on the structure of the Taupo Volcanic Zone and its hydrothermal circulation.
Journal of volcanology and geothermal research. 1995;68(1-3):29–58.
 168. Druitt TH, Edwards L, Mellors R, Pyle D, Sparks R, Lanphere M, et al.
Santorini volcano. vol. 19 of Geological Society Memoir.
Geological Society of London; 1999.
 169. Pyle DM, Elliott JR.
Quantitative morphology, recent evolution, and future activity of the Kameni Islands volcano, Santorini, Greece.
Geosphere. 2006;2(5):253–268.
 170. Nomikou P, Parks M, Papanikolaou D, Pyle D, Mather T, Carey S, et al.
The emergence and growth of a submarine volcano: The Kameni islands, Santorini (Greece).
GeoResJ. 2014;1:8–18.
 171. Newman AV, Stiros S, Feng L, Psimoulis P, Moschas F, Saltogianni V, et al.
Recent geodetic unrest at Santorini caldera, Greece.
Geophysical Research Letters. 2012;39(6).
 172. Parks MM, Biggs J, England P, Mather TA, Nomikou P, Palamartchouk K, et al.
Evolution of Santorini Volcano dominated by episodic and rapid fluxes of melt from depth.
Nature Geoscience. 2012;5(10):749.
 173. Parks MM, Caliro S, Chiodini G, Pyle DM, Mather TA, Berlo K, et al.
Distinguishing contributions to diffuse CO₂ emissions in volcanic areas from magmatic degassing and thermal decarbonation using soil gas ²²²Rn–^δ13C systematics: Application to Santorini volcano, Greece.
Earth and Planetary Science Letters. 2013;377:180–190.
 174. Druitt T, Mercier M, Florentin L, Deloule E, Cluzel N, Flaherty T, et al.
Magma storage and extraction associated with Plinian and Interplinian activity at Santorini caldera (Greece).
Journal of Petrology. 2016;57(3):461–494.

175. Tassi F, Vaselli O, Papazachos C, Giannini L, Chiodini G, Vougioukalakis G, et al.
Geochemical and isotopic changes in the fumarolic and submerged gas discharges during the 2011–2012 unrest at Santorini caldera (Greece).
Bulletin of Volcanology. 2013;75(4):711.
176. Rizzo A, Barberi F, Carapezza M, Di Piazza A, Francalanci L, Sortino F, et al.
New mafic magma refilling a quiescent volcano: Evidence from He-Ne-Ar isotopes during the 2011–2012 unrest at Santorini, Greece.
Geochemistry, Geophysics, Geosystems. 2015;16(3):798–814.
177. Bohnenstiehl D, Tolstoy M, Dziak R, Fox C, Smith D.
Aftershock sequences in the mid-ocean ridge environment: An analysis using hydroacoustic data.
Tectonophysics. 2002;354(1-2):49–70.
178. Sohn RA, Hildebrand JA, Webb SC.
A microearthquake survey of the high-temperature vent fields on the volcanically active East Pacific Rise (9°N–50°N).
Journal of Geophysical Research: Solid Earth. 1999;104(B11):25367–25377.
179. Germanovich LN, Lowell RP, Ramondenc P.
Magmatic origin of hydrothermal response to earthquake swarms: Constraints from heat flow and geochemical data.
Journal of Geophysical Research: Solid Earth. 2011;116(B5).
180. Anderson K, Segall P.
Physics-based models of ground deformation and extrusion rate at effusively erupting volcanoes.
Journal of Geophysical Research: Solid Earth. 2011;116(B7).
181. Cashman K, Biggs J.
Common processes at unique volcanoes – a volcanological conundrum.
Frontiers in Earth Science. 2014;2:28.
182. Montgomery-Brown E, Wicks C, Cervelli PF, Langbein JO, Svarc JL, Shelly DR, et al.
Renewed inflation of Long Valley Caldera, California (2011 to 2014).
Geophysical Research Letters. 2015;42(13):5250–5257.
183. Del Gaudio C, Aquino I, Ricciardi G, Ricco C, Scandone R.
Unrest episodes at Campi Flegrei: A reconstruction of vertical ground movements during 1905–2009.
Journal of Volcanology and Geothermal Research. 2010;195(1):48–56.
184. Smith RB, Jordan M, Steinberger B, Puskas CM, Farrell J, Waite GP, et al.
Geodynamics of the Yellowstone hotspot and mantle plume: Seismic and GPS imaging, kinematics, and mantle flow.
Journal of Volcanology and Geothermal Research. 2009;188(1-3):26–56.
185. Yang XM, Davis PM, Dieterich JH.
Deformation from inflation of a dipping finite prolate spheroid in an elastic half-space as a model for volcanic stressing.
J Geophys Res. 1988;93:4249–4257.
186. Constantinescu R, Robertson R, Lindsay JM, Tonini R, Sandri L, Rouwet D, et al.
Application of the probabilistic model BET_UNREST during a volcanic unrest simulation exercise in Dominica, Lesser Antilles.
Geochemistry, Geophysics, Geosystems. 2016;17(11):4438–4456.
187. McNutt SR, Tytgat G, Power J.
Preliminary analyses of volcanic tremor associated with the 1992 eruptions of Crater Peak, Mt. Spurr, Alaska.
US Geological Survey Bulletin 2139. 1995;2139:161.
188. Power J, Jolly A, Nye C, Harbin M.
A conceptual model of the Mount Spurr magmatic system from seismic and geochemical observations of the 1992 Crater Peak eruption sequence.
Bulletin of volcanology. 2002;64(3-4):206–218.
189. Power JA, Lalla DJ.
Seismic observations of Augustine Volcano, 1970–2007.
US Geological Survey Professional Paper 1769. 2010;p. 3–40.
190. McNutt SR, Tytgat G, Estes SA, Stihler SD.

- A parametric study of the January 2006 explosive eruptions of Augustine Volcano, using seismic, infrasonic, and lightning data.
US Geological Survey Professional Paper 1769. 2010;p. 85–102.
191. Ukawa M.
Excitation mechanism of large-amplitude volcanic tremor associated with the 1989 Ito-oki submarine eruption, central Japan.
Journal of volcanology and geothermal research. 1993;55(1-2):33–50.
 192. Endo ET, Malone SD, Noson LL, Weaver C.
Locations, magnitudes, and statistics of the March 20–May 18 earthquake sequence.
US Geol Surv Prof Pap. 1981;1250:93–107.
 193. Scandone R, Malone SD.
Magma supply, magma discharge and readjustment of the feeding system of Mount St. Helens during 1980.
Journal of Volcanology and Geothermal Research. 1985;23(3-4):239–262.
 194. Frémont MJ, Malone SD.
High precision relative locations of earthquakes at Mount St. Helens, Washington.
Journal of Geophysical Research: Solid Earth. 1987;92(B10):10223–10236.
 195. McNutt SR, Beavan R.
Patterns of earthquakes and the effect of solid earth and ocean load tides at Mount St. Helens prior to the May 18, 1980, eruption.
Journal of Geophysical Research: Solid Earth. 1984;89(B5):3075–3086.

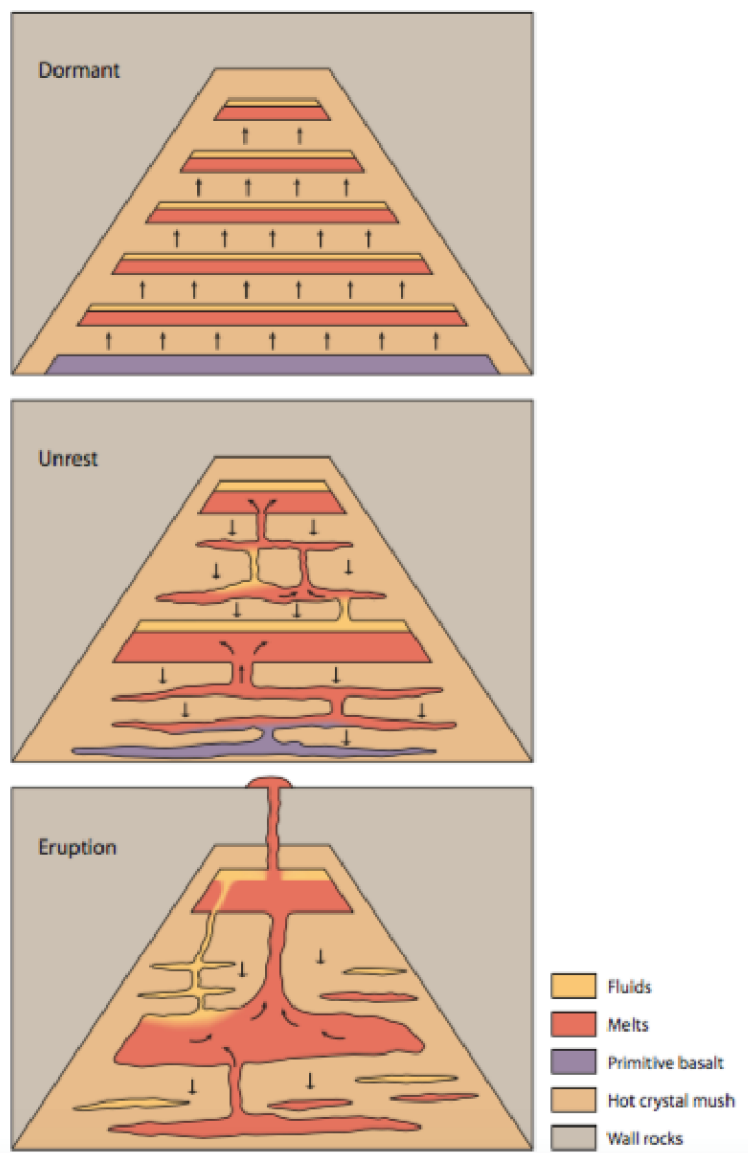


Figure 1. Cartoon of the trans-crustal magmatic system (TCMS) model of a volcano showing multiple layers of different compositions: primitive basalt magma (purple); layers of fractionated melt (dark orange); magmatic fluids/volatiles (yellow); crystal-dominated framework (mush; pale orange); and surrounding country rock (grey). The panels show three different states of activity: (top) Dormant period with background activity (e.g., fumaroles, low level deformation and seismicity). (middle) Unrest state: destabilization of layers of melt and magmatic fluids connect and move upward. (bottom) Major destabilization of the TCMS leads to eruption of magma. Used with permission from: [1].

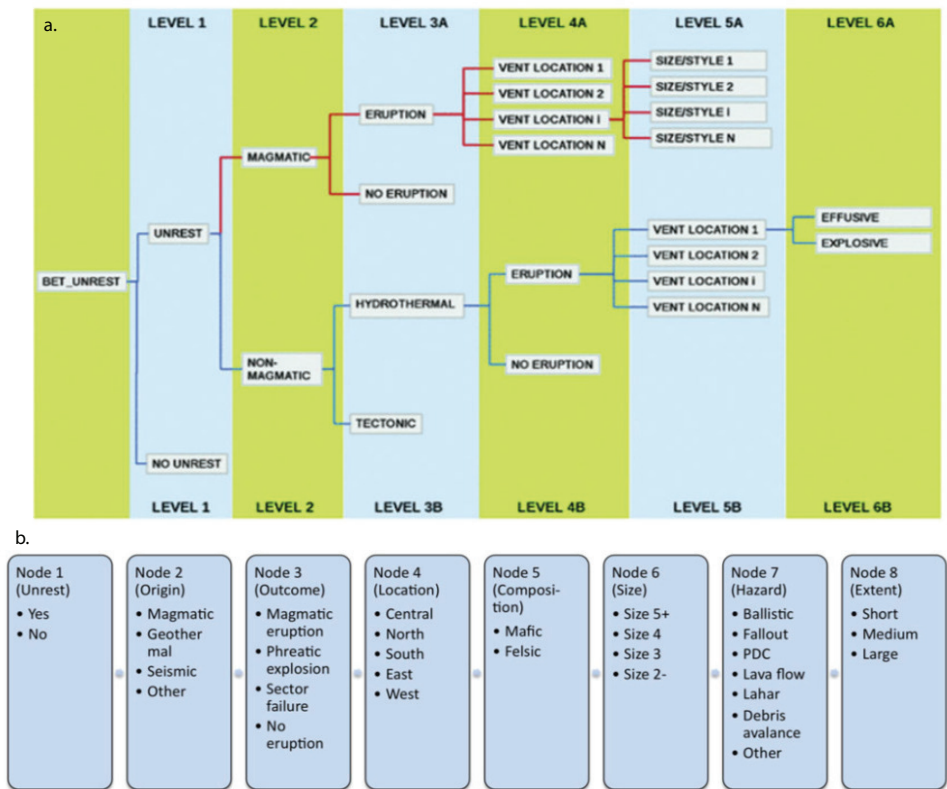


Figure 2. Examples of two different Bayesian Event Trees (BETs) that incorporate assessment of the origin of unrest. a. From Sandri et al., (2017) [13] distributed under the Creative Commons Attribution 4.0 International License (<http://creativecommons.org/licenses/by/4.0/>) with no changes made. b. From Sobradelo et al. (2014) [12] which is under the Creative Commons Attribution License.

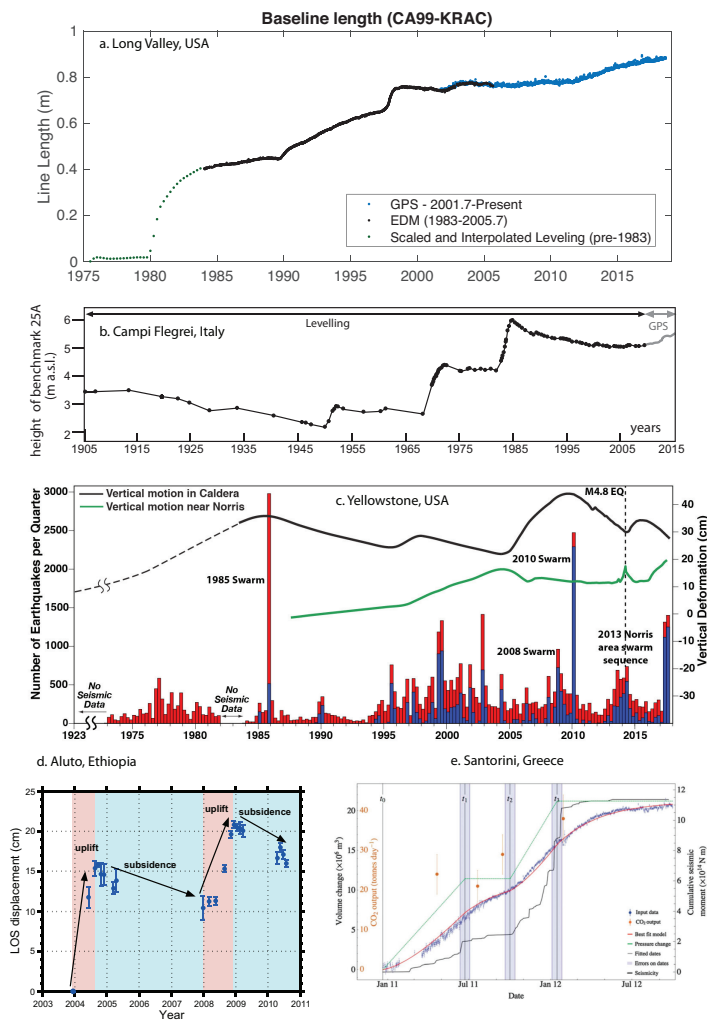


Figure 3. Time series of deformation (and other datasets, where available) spanning multiple decades at restless calderas near the locations of maximum displacement. (a) Time series of caldera deformation from Electronic Distance Measurements (EDM) line length change, leveling, and GPS at Long Valley, USA showing about 80 cm of expansion, shown as line length increase between the measurement points at CA99 and KRAC (including uplift with little subsidence) updated from [182] by Emily Montgomery-Brown. (b) Time series of vertical deformation at Campi Flegrei, Italy from leveling and GPS showing uplift with some subsidence modified from [15] courtesy of Valerio Accocella. Original leveling data are from [183] and GPS data are from Observatorio Vesuviano. (c) Vertical deformation time series at Yellowstone, USA in two locations (Norris Geyser Basin and Sour Creek Dome) showing that uplift and subsidence measured by leveling and GPS are often anti-correlated at these two locations. A change from subsidence to uplift in one area is associated with a change in deformation in the opposite direction in the other location. Sometimes the changes happen very rapidly, as in the spike in deformation in 2014 shown by vertical dashed line (related to an earthquake swarm that started in 2013). Figure updated from [184] courtesy of Jaime Farrell. Earthquake swarms (blue bars) and all earthquakes (red bars) in the area are also shown. (d) Time series of deformation in the InSAR line-of-sight (LOS) at Aluto caldera modified from [153] courtesy of Will Hutchison. (e) Time series at Santorini showing seismicity, CO₂ degassing flux from near the summit of Nea Kameni, deformation (from GPS) and numerical model from [59]. Vertical lines labeled t_0 , t_1 , t_2 and t_3 are the time periods when the numerical model has a change in the pressure function.

Cordón Caulle

32

rst.a.royalsocietypublishing.org Phil. Trans. R. Soc00000000

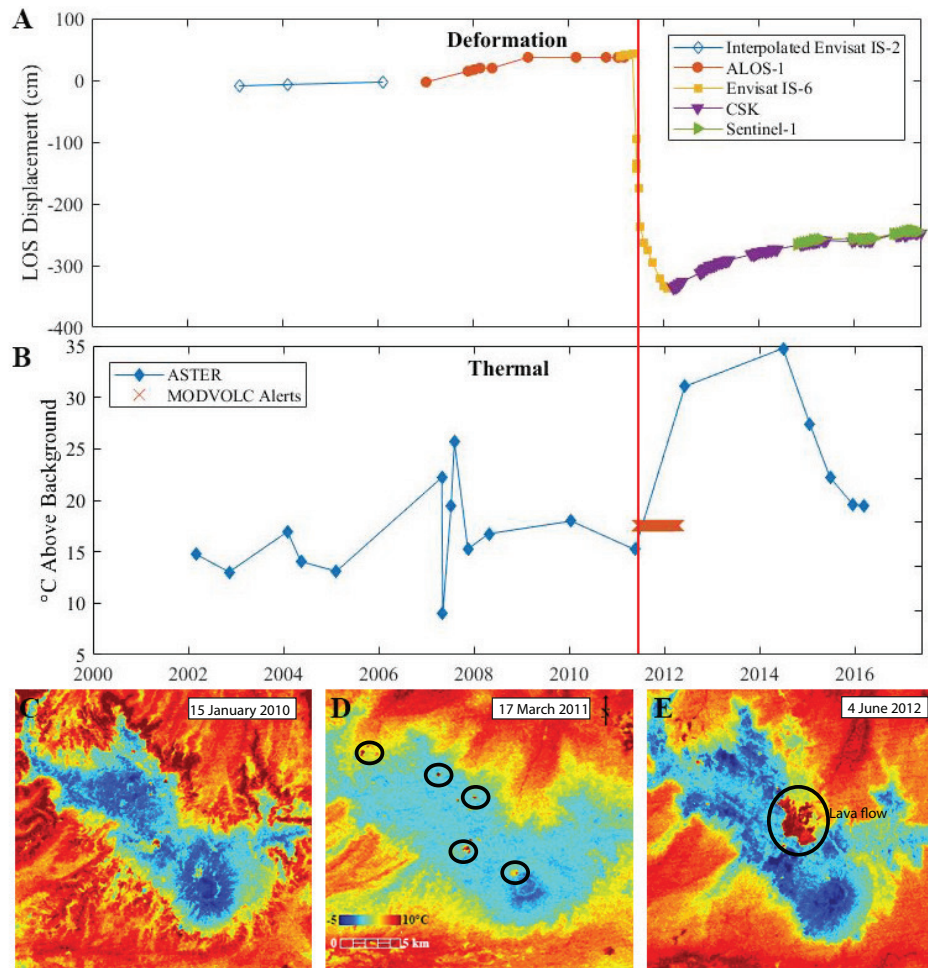


Figure 4. Satellite deformation and temperature time series for Cordón Caulle volcano, Chile. (a) Time series of ground displacement measured from InSAR in the radar line-of-sight (LOS) from several different satellites. CSK (COSMO-SkyMed, Italian Space Agency) and Sentinel-1 (European Space Agency) datasets [60] were collected from the points: CSK: -40.492, -72.211; Sentinel: -40.495, -72.185. ALOS-1 (Advanced Land Observing Satellite, Japanese Space Agency) data [145] and Envisat (European Space Agency) 2003-2006 [17] are maximum rates of deformation. Envisat data from 6/1/11 to 3/13/12 generated through the use of a Yang model [185] to predict the deformation at the crater due to decorrelation surrounding the main vent during the eruption caused by flows. All datasets with open points are interpolated from the general displacement trend of the data and do not represent the measured displacement values of the data points. (b) Time series of hottest temperature above background for fumaroles at Cordón Caulle (see C-E) as measured by the ASTER sensor on the Terra satellite using the method of [18]. After the ASTER acquisition on 5/17/2011, the hottest thermal anomaly shifts from the previously active geothermal areas to the newly generated vent of the 6/4/2011 eruption. C-D are ASTER TIR images with the same spatial and temperature scale. Locations of fumarole areas are circled. Temperatures values are in °C above background. Images were acquired (c) 15 January 2010, (d) 17 March 2011 (before the eruption), and (e) 4 June 2012 (after the eruption). A and B modified from Reath et al., (submitted). Vertical red line represents the timing of the $\sim 1.5\text{km}^3$ dense rock equivalent explosive-effusive rhyodacite eruption onset (11 June 2011) that lasted until March 2012.

Table 1. Examples of criteria used at three volcanoes by Sandri et al., (2017) [13] to distinguish non-magmatic unrest. Y/N means that the criteria is whether the the phenomena have been observed (yes/no). Information on the numeric probabilities is not available.

Popocatépetl	Cotopaxi	Dominica
incandescence of dome (Y/N)	SO ₂ flux (> 100-350 t/d)	C/S up or down after up (Y/N)
Duration of tremor > 6000s	fumarole temperature increase > 119°C	HCl ¹ , HF, SO ₂ detected
SO ₂ flux (> 2000 t/d)	EQ depth (> 4.5-5.5 km)	temperature increase > 300°C
	Existence of deep VLP (Y/N)	Any VLPs (Y/N)
	acidic gases (Y/N)	# LPs after significant VT swarms (#/day > 5-10)
	VT/month (> 32)	Consistent increase in # of VTs for 1 month (Y/N)
	Harmonic LP tremor (Y/N)	Deep VTs (#/week > 4-5)
	increased deformation rates (Y/N)	Detectable radial deformation (Y/N)
	VLP and LP together (Y/N)	Surface deformation (island wide, >6 cm in 6 months)

Table 2: Proposed check list for determining cause of volcanic unrest – the columns labeled "If (non-)magmatic" specify how each observation would be manifest if the unrest was magmatic or not. In the column of examples, (M) means that a magmatic source of unrest has been proposed using a given observation, (NM) means a non-magmatic source of unrest and (B) means both. In several cases the interpretation for the cause of unrest is controversial, see main text for discussion. Examples selected are discussed in the main text (or see references given) and are not intended to be complete.

Observation	Complications	If magmatic	If non-magmatic	Examples
Geomorphology (uplift/subsidence over 100 years or longer)	Non-volcanic sources of uplift/subsidence; deformation source moves laterally	Repeated intrusions build topography	No net deformation when only fluid movements (although see [44])	Uturuncu (NM), Lazufre (B), Laguna del Maule (M), Ioto (Iwo Jima) (M) [41]
Gravity change	Other sources of gravity change (e.g., groundwater)	density change $> 2500 \text{ kg m}^{-3}$; gravity increase without deformation	density change $< 1115 \text{ kg m}^{-3}$	Long Valley (M), Kilauea (M) [28], Yellowstone (B), Uturuncu (NM), Corbetti (M) [29], Laguna Del Maule (B)
Seismic swarm characteristics: 1) tremor reduced displacement	1) some overlap and also depth dependence	1) larger amplitude ($> 5 \text{ cm}^2$)	1) small amplitude ($< 5 \text{ cm}^2$)	1) Spurr (M) [83,187,188]
2) b-value	2) non-unique	2) decrease for higher stress	2) increase for higher pore pressure	2) Augustine (M) [79,189,190]
3) generic swarm sequence: VT, quiescence, LF, tremor, eruption	3) rates quite variable	3) Whole sequence, eruptions more likely	3) VT only, eruptions less likely	3) Off Ito (M) [191,191], Mt. St. Helens (M) [192–195]
4) depth	4) some overlap	4) deeper	4) shallower	4) Spurr (M) [83,187,188], Augustine (M) [79,189,190]
5) lateral propagation speed	4) some overlap	4) fast (several km/day)	4) slower	5) Jailolo [80] (M)

Rate of change of ground deformation	non-unique	Rapid onset of uplift requires magma? [14]	Fast change from uplift-subsidence requires low viscosity fluid	Yellowstone (B), Aluto (B)
$^3\text{He}/^4\text{He}$ ratio	Other explanations are possible	Increase (>3 Ra) implies magmatic source	Less change	Santorini (M)
CO_2 flux	Time consuming to measure over large area	Large increase in flux from magma intrusion, especially mafic	Changes in flux do not require new magma	Mammoth Mountain (M), Campi Flegrei (M)
$\text{H}_2\text{O}_{(\text{f})}/\text{CO}_{2(\text{f})}$ ratio	Non-unique	Increase from shallow magma intrusion, especially mafic	Changes in ratio do not require new magma	Campi Flegrei (M)
CO_2/SO_2 and $\text{H}_2\text{S}/\text{SO}_2$ ratios	Can get hydrothermal system scrubbing or P, T conditions causing change, not new magma; Few measurements available	Increase due to influx of new magma at depth	No change or decrease	Poás (M) [91], Villarrica (M) [92], Merapi (M) [95]
$\delta^{13}\text{C}-\text{CO}_2$ isotopic composition	Other explanations possible	-4 to -8 ‰ suggest deep magmatic source	Smaller change	Santorini (M), Aluto (M)
$\text{H}_2/\text{H}_2\text{O}$ ratio	Other explanations possible	Increase could be caused by temperature increase from new magma	Could change in smaller or opposite ways	Santorini (M)
HCl, CO, H_2 , Radon, CH_4	Few measurements available, other explanations possible	Changes can indicate new magma	Less change	Merapi (M) [95], Santorini (M)
Surface hydrothermal system	Hydrothermal system could be offset from volcano or area of unrest or a hidden system is possible	When absent, unrest is primarily magmatic (unless hydrothermal system is blind)	When present, non-magmatic source should be considered	Laguna del Maule (M); Lastarria-Lazufre (B)

Depth of ground deformation	Need to carefully test depth sensitivity	Source deeper than hydrothermal system	Source overlaps with hydrothermal system	Uturuncu (M), Cordon Caulle (M)
Surface temperature	Can be masked by near-surface fluid flow	Extreme temperature increase (e.g., incandescence): magma near surface	Change or no change both permitted	Popocatepetl (M) [13], Villarrica (M) [69]
SO ₂ flux	Non-unique (e.g., reduce flux through scrubbing by hydrothermal system)	Increase: new magma intrusion (or less scrubbing as hydrothermal system boiled away)	Less change	Pinatubo (M)